



1 **Comparison of statistical and analytical hierarchy process methods on flood susceptibility**  
2 **mapping: in a case study of Tana sub-basin in northwestern Ethiopia**

3 Azemeraw Wubalem<sup>\*1</sup>, Gashaw Tesfaw<sup>1</sup>, Zerihun Dawit<sup>1</sup>, Belete Getahun<sup>1</sup>, Tamirat  
4 Mekuria<sup>1</sup>, Muralitharan Jothimani<sup>1</sup>

5 1. Department of Geology, College of Natural and Computational Sciences, University of Gondar,  
6 Ethiopia, P.X.BOX 196

7 **Abstract:** The sub-basin of Lake Tana is one of the most flood-prone areas in northwestern  
8 Ethiopia, which is affected by flood hazards. Flood susceptibility modeling in this area is essential  
9 for hazard reduction purposes. For this, the analytical hierarchy process (AHP), bivariate, and  
10 multivariate statistical methods were used. Using an intensive field survey, historical record, and  
11 Google Earth Imagery, 1404 flood locations were determined which are classified into 70%  
12 training datasets and 30% testing flood datasets using subset in the GIS tool. The statistical  
13 relationship between the probability of flood occurrence and eleven flood-driving factors is  
14 performed using the GIS tool. Then, the flood susceptibility map of the area is developed by  
15 summing all weighted factors using a raster calculator and classified into very low, low, moderate,  
16 high, and very high susceptibility classes using the natural breaks method. The results for the area  
17 under the curve (AUC) are 99.1% for the frequency ratio model is better than 86.9% using AHP,  
18 81.4% using the logistic regression model, and 78.2% using the information value model. Based  
19 on the AUC values, the frequency ratio (FR) model is relatively better followed by the AHP model  
20 for regional flood use planning, flood hazard mitigation, and prevention purposes.

21 **Keywords:** *flood, susceptibility, Geographic Information System (GIS), analytical hierarchy*  
22 *process (AHP), frequency ratio, information value, logistic regression, Ethiopia*

23

24 **Introduction**

25 A flood is an overflow of water that submerges usually dry land. It can also occur in rivers or lakes  
26 when the flow rate exceeds the capacity of rivers channel, particularly at the bends or meanders in  
27 the waterway and backflow from the Lakes. Natural hazards, in particular flood, has been affecting  
28 the world during rainy seasons. Even though Flood is one of the natural parts of the hydrological  
29 cycle, it is increased in both frequency and magnitude from year to year. This is because of the  
30 over change of climate and land degradation on the Earth due to the anthropogenic intervention.



31 The anthropogenic intervention on the Earth can reduce the water retention capacity of the  
32 catchments because of the cleanup of forestation for a different purpose, which resulted in a high  
33 rate of soil erosions. The Flood hazard has been causing damage to crops, infrastructures,  
34 engineering structures, properties, and loss of human and animal lives worldwide including  
35 Ethiopia. As reported by (Samanta et al., 201; Calil et al. 2015), the flood has resulted in a risk to  
36 a human being (like loss of life, injury), properties (agricultural area, yield production, villages,  
37 and buildings), communication systems (urban infrastructure, bridges, roads, and railway routes),  
38 cultural heritage and ecosystems. (Zou et al., 2013; Calil et al., 2015) stated that more than 2000  
39 deaths can occur within a single year and more than 75 million people have adversely affected  
40 across the planet Earth by flood hazards.

41 Flood hazard is becoming one of the destructive natural hazards in Ethiopia followed by landslide  
42 incidences and resulted in huge damages of properties, crops, farmlands, infrastructures, and loss  
43 of life. For example, in the last two years, 2019-2020, flood hazard was displaced more than  
44 500,000 people and damaged wide cultivated lands (more than 25, 000 ha cultivated lands),  
45 damaged various engineering structures, destructed more than 35 houses, and loss of lives in  
46 Amhara, Somali, Afar, SNNP, Dire Dwa, and Oromia regions of Ethiopia. The study area is one  
47 of the severely affected areas by flooding which resulted in the loss of life, properties, destruction  
48 of houses, roads, and more than 7, 000-hectare farmlands covered by various crops in the area.  
49 These show that huge economic loss caused by flooding hazard that retards the sustainable  
50 development of the economy of the country. Therefore, flood susceptibility mapping is one of the  
51 most important elements for early warning systems or strategies to prevent and mitigate future  
52 flood situation, which helps to reduce the negative results of flood hazard. Flood susceptibility  
53 mapping can be also perceived as one of the ways of vulnerability assessment (Adger et al., 2006;  
54 Jacinto et al. 2015). In geohazard mapping, susceptibility/vulnerability, hazard and risk mapping  
55 are the most important activities to understand, mapping and evaluating the spatiotemporal  
56 condition and level of risk due to geohazards. These terms have different meanings but some  
57 researchers use the terms interchangeably. Susceptibility refers to the probability of occurrence of  
58 an event within particular type in a given location where as hazard refers the probability of  
59 occurrence of an event within a particular type and magnitude in a given location within a reference  
60 period. This means, susceptibility can be used to predict the spatial occurrence of an events, but



61 hazard can be used to predict the spatiotemporal occurrence of an events in a given terrain. The  
62 term risk refers to the expected losses or damage by an events in a given regions which is the  
63 products of susceptibility, hazard and elements at risk. Hence, the main objective of this study is  
64 to prepare flood susceptibility map, this study only focus on flood susceptibility other than hazard  
65 and risk. The flood susceptibility mapping has implementing using various methods by different  
66 and numerous studies. These methods including qualitative (for example, analytical hierarchy  
67 process (AHP), quantitative (machine learning, statistical), and hydrological based methods. The  
68 hydrological methods are very simple and are based on a nonlinear concept and they are less  
69 effective to model complex features like catchments (Sahoo et al., 2009). Nowadays, these  
70 traditional methods have been replaced by automated and rule-based methods that are more  
71 suitable for flood hazard mapping (Hostache et al., 2013). SWAT (Anjum et al., 2016) and  
72 WetSpss (Nurmohamed et al., 2012) methods are examples of hydrological methods that are used  
73 to produced spatial flood susceptibility models by integrated GIS and remote sensing tools.  
74 Qualitative methods are an expert-driven approach, which required field experience specialists  
75 (Rahmati et al., 2016; Dahri and Abida 2017). Rely on the experience and professional background  
76 knowledge of experts and subjectivity is the drawback of these methods. An analytical hierarchy  
77 process (AHP) is an example of a qualitative method used by many scholars to produce a flood  
78 susceptibility model based on a multicriteria analysis framework (Karimi et al., 2018). Machine  
79 learning techniques are advanced methods that used in flood susceptibility mapping, however, a  
80 considerable processing time, the requirement of having high-performance computing systems  
81 along with specific software, and strict selection criteria for input parameters make machine  
82 learning methods less usable for a wide range of users (Ghalkhani et al., 2013; Tehrany et al. 2013).  
83 Statistical methods are indirect susceptibility mapping methods widely or routinely used to  
84 evaluate the correlation between flood driving factors and floods based on mathematical  
85 expression (Bednarik et al., 2012; Chen and Wang, 2007; Pradhan et al., 2011; Regmi et al., 2014;  
86 Wang et al., 2011). Statistical methods are imperative to utilize quick, understandable, and  
87 accurate methods for flood susceptibility modeling. It has no specific requirements regarding input  
88 data, software, and computer capacity. The statistical methods can be further divided into  
89 multivariate and bivariate statistical methods, which are widely used throughout the world. They  
90 provide reliable results (Dai and Lepcha, 2002; Donati and Turrini, 2002; Luelseged and  
91 Yamagishi, 2005; Duman et al., 2006; Sarkar et al., 2013; Meten et al., 2015; Chandak et al., 2016;



92 Kouhpeima et al., 2017; Wubalem and Meten, 2020; Hong et al., 2020). The bivariate statistical  
93 methods are used to evaluate the relationship between flood governing factors and past flooding.  
94 Frequency ratio, certainty factor, information value, and weight of evidence are examples of  
95 bivariate statistical methods, which are simple, easy, and produce reliable models. It also helps to  
96 evaluate the effects of a flood at a factor class level that is impossible in data mining or multivariate  
97 methods. However, it requires quality input data, past flood data, and lacking to evaluate the  
98 relationship among flood governing factors. Multivariate statistical methods are used to examine  
99 the relationship between three and above dependent and independent variables (Pham et al., 2016b;  
100 Das, 2019; Duman et al., 2006; Kouhpeima et al., 2017; Luelseged and Yamagishi, 2005). Logistic  
101 regression and discriminant analysis are examples of multivariate statistical methods used  
102 frequently in flood susceptibility modeling and provide reliable results (Chen and Wang, 2007;  
103 Das, 2019; Duman et al., 2006; Kouhpeima et al., 2017; Luelseged and Yamagishi, 2005; Meten  
104 et al., 2015). However, it is incapable to examine the contribution of each factor class for flood  
105 probability like data mining, unlike bivariate methods.

106 Many scholars have been employing both qualitative and quantitative methods for flood  
107 susceptibility modeling, however, no clear and tangible agreements to select the best methods for  
108 flood susceptibility modeling practice. Although the suitability of the model depend on various  
109 constraints including physical parameters, data quality and availability, expert and technological  
110 advancement, comparison among different natural hazard mapping methods is one of the solution  
111 to select appropriate approaches. Hence, each methods has its own limitation, using different  
112 approaches together for landslide or flood susceptibility mapping is very important to fill the gap  
113 among the methods. For example, the logistic regression model can perform multivariate statistical  
114 analysis between a dependent variable and a set of independent variables, but it is incapable to  
115 analyze the impacts of internal classes of flood governing factors individually on flood occurrence.  
116 This limitation can be solved using bivariate statistical methods, for example, frequency ratio and  
117 information value statistical methods can be extracted the influence of each flood governing factor  
118 class on flood occurrence, but it cannot consider the relationship between these flood governing  
119 factors and flood occurrence. Therefore, a combination use of bivariate and multivariate statistical  
120 methods are very essential to overcome the limitation of each methods. As a result, in the present  
121 study, bivariate, multivariate and expert methods are employed to generate flood susceptibility



122 model in sub basin of Lake Tana and the performance of each methods has been evaluated using  
123 receiver operating characteristics curve and area under the curve (AUC). Thus, based on the  
124 concerns stated overhead, the main objective of this study is 1) to compare and evaluate the  
125 performance of the frequency ratio, information value, logistic regression and analytical hierarchy  
126 process methods to determine flood prone areas 2) to evaluate the relationship between flood  
127 factors and flood probability as well as flood factor class and flood occurrence probability. The  
128 nobility of this study lies on, 1) for the first time, the rigorous flood susceptibility methods like  
129 statistical methods was conducted in the sub basin of Lake Tana to generate flood susceptibility  
130 model 2) the comparison among the information value, frequency ratio, logistic regression and  
131 analytical hierarchy process methods has not performed yet. This study will be determined  
132 statistically significant methods for flood susceptibility modeling. The resulted map will be helped  
133 the regional and local authorities and policy makers to mitigate flood hazards.

## 134 Study Area

135 The study area is located in Amhara Regional State of the sub-basin of Lake Tana basin in  
136 northwestern Ethiopia, which is characterized, by wide flat to gently sloping plains and somehow  
137 rugged topography. Its elevation ranges from 1,774-4,037 m above mean sea level (Fig. 1). It is  
138 bound between 330,000-410, 000 E and 1,280,000-1,350,000 N. It is characterized by subtropical  
139 to cool climatically zones with very high and prolonged rainfall in between Jun to October. The  
140 study area is covered mainly three Districts including Fogera, Farta, and Libo Kemkem which is  
141 frequently affected by flood hazards yearly during heavy and prolonged rainfall seasons. The study  
142 area has many tributaries that drained to the two major rivers called Gumara and Ribb Rivers that  
143 also drained to Lake Tana, which is the parts of the Abay basin. Agriculture is one of the most  
144 dominant land use in the study area, which is performed more than two per year. The dominant  
145 soil types in the study area including clay, loam, sandy loam, silty sand, fine to coarse sand, and  
146 gravels sourced from volcanic rocks.

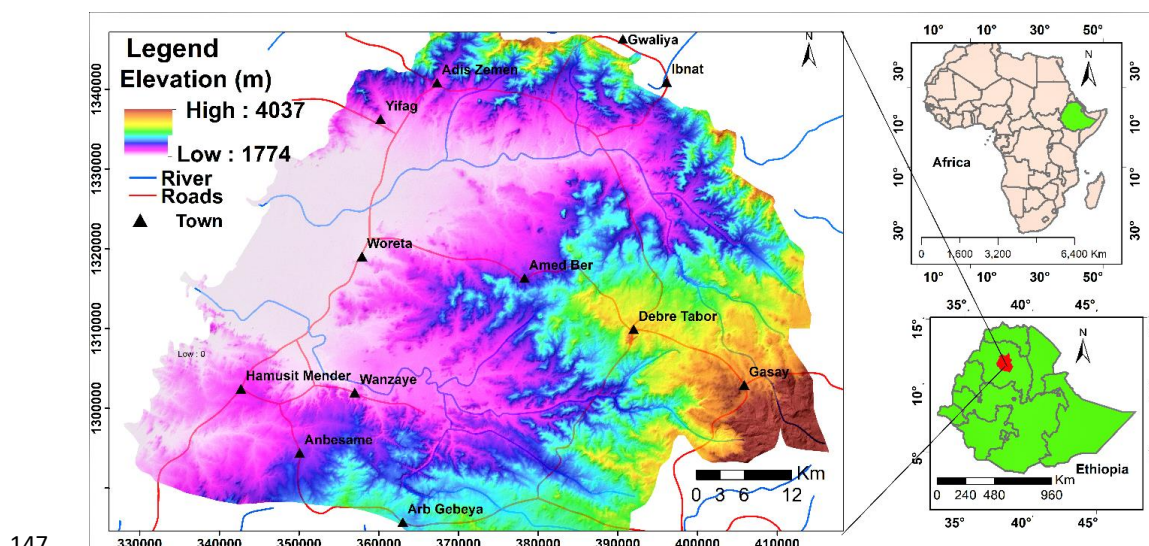


Figure 1 Location Map of the Study Area

## Data Used

### Flood Inventory Map

In flood susceptibility mapping, flood inventory mapping is one of the key element, which can be prepared using various techniques like the aerial photograph or Google Earth Imagery interpretation, field investigation, and evaluation of archived data coupled with GIS tool. Evaluating and recognizing the correlation between flood driving factors and flood incidences is required an accurate and precise flood inventory map (Pradhan et al., 2012; Tehrany and Jones, 2017; Mahyat et al., 2019). This flood inventory map can be prepared in map forms from the data that can be collected from a satellite image or Google Earth Imagery interpretation, historical records, and extensive field survey. In the present research work, 1404 most relevant flood inventory data were collected from historical records, Google Earth Imagery interpretation, and Extensive fieldwork (Fig. 2). In the literature, several suggestions are provided regarding the size of flood samples to be used for modeling and model verification (Ohlmacher and Davis, 2003). Therefore, based on a literature review, the flood inventory data was classified into 70% (983) flood for the training dataset and 30% (421) for testing datasets keeping their spatial distribution using subset in ArcGIS 10.1 (Lee et al., 2012; Tehrany et al., 2013; Khosravi et al., 2016; Mahyat





et al., 2019) as shown in the figure. The same number of flood and non-flood points were chosen for the logistic regression analysis.

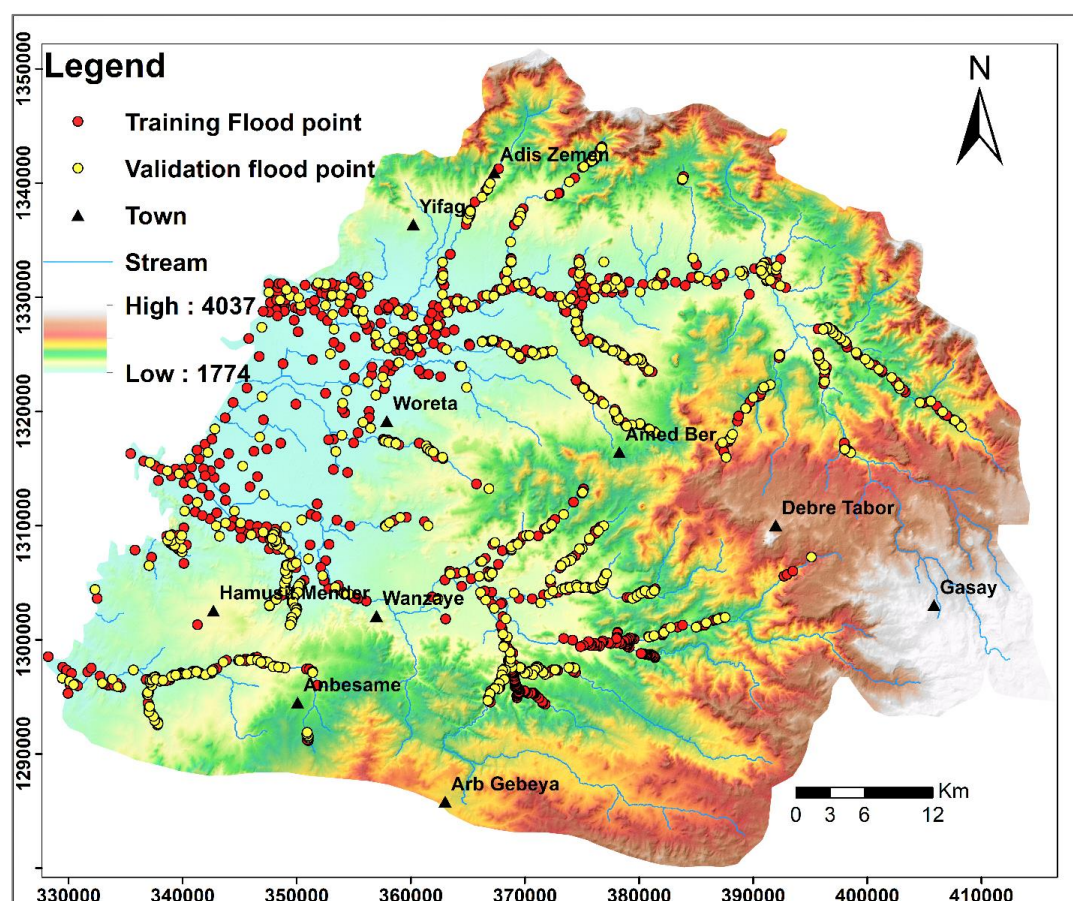


Figure 2 Flood location map

## Flood Driving Factors

The selection of flood factors is one of the most crucial elements in flood susceptibility mapping, which depend on physical and natural characteristics of the study area and data availability (Kia et al., 2012; Liuzzo et al., 2019), however, no well-defined standards to select the most significant flood driving factors. The factors that initiate the flood incidence in the study area are selected based on the study area's environmental condition, data availability, logistic regression analysis,



176 and a literature review (Lee et al, 2012; Mahyat et al., 2019). The slope angle, slope curvature,  
177 land use, soil texture, distance to stream/river, stream density, normalized vegetation index, flow  
178 accumulation, groundwater depth, rainfall, and elevation have taken into account to examine the  
179 spatial relationship between them and flood occurrence in the study area. These factors were  
180 classified into subfactor classes using a natural break in ArcGIS to evaluate the effects of each  
181 flood factor class for the case of frequency ratio and information value methods. The flood factors,  
182 which have derived from DEM, distance to stream (five classes), slope angle (five classes), flow  
183 accumulation (five classes), stream density (five classes), elevation (five classes), and slope  
184 curvature (three classes) maps were constructed from 12.5 m x 12.5 m resolution DEM (Fig. 3).  
185 The soil map of the study area is prepared through digitization from a 1:50,000 textural soil map  
186 of the Amhara Region, which has four classes (silty sand, sandy loam, clay, and loam). Land use  
187 and NDVI maps of the study area were prepared from Sentinel 2 satellite image analysis using  
188 ArcGIS with the help of high-resolution Google Earth image interpretation. The LULC has eight  
189 classes including grazing land, agricultural land, barren land, residential/settlement, river zone  
190 /water body, dense forest, moderate forest, and wetland (Fig. 3) whereas NDVI has five classes.  
191 The rainfall and groundwater depth raster map was constructed using ArcGIS 10.1 from annual  
192 mean rainfall and well data that are collected from Amhara Metrological Agency and Amhara  
193 Water Well Drilling Enterprise, respectively. To determine the effects of each flood factor class  
194 on flood occurrence, weight rating through flood factor raster combined with flood raster map is  
195 important. For this purpose, all flood factor maps converted into a raster and reclassified with the  
196 same pixel size (12.5 m x 12.5 m) and the same projection using the GIS tool. Then, the flood  
197 inventory map is overlaid through a combination of spatial analysis tools under the local toolbox  
198 with flood factor raster class to extracted flood pixels for each flood driving factor class. Then the  
199 effects of each factor class were determined using the equation of frequency ratio, and information  
200 value methods as summarized in Table 1.

201

202

203



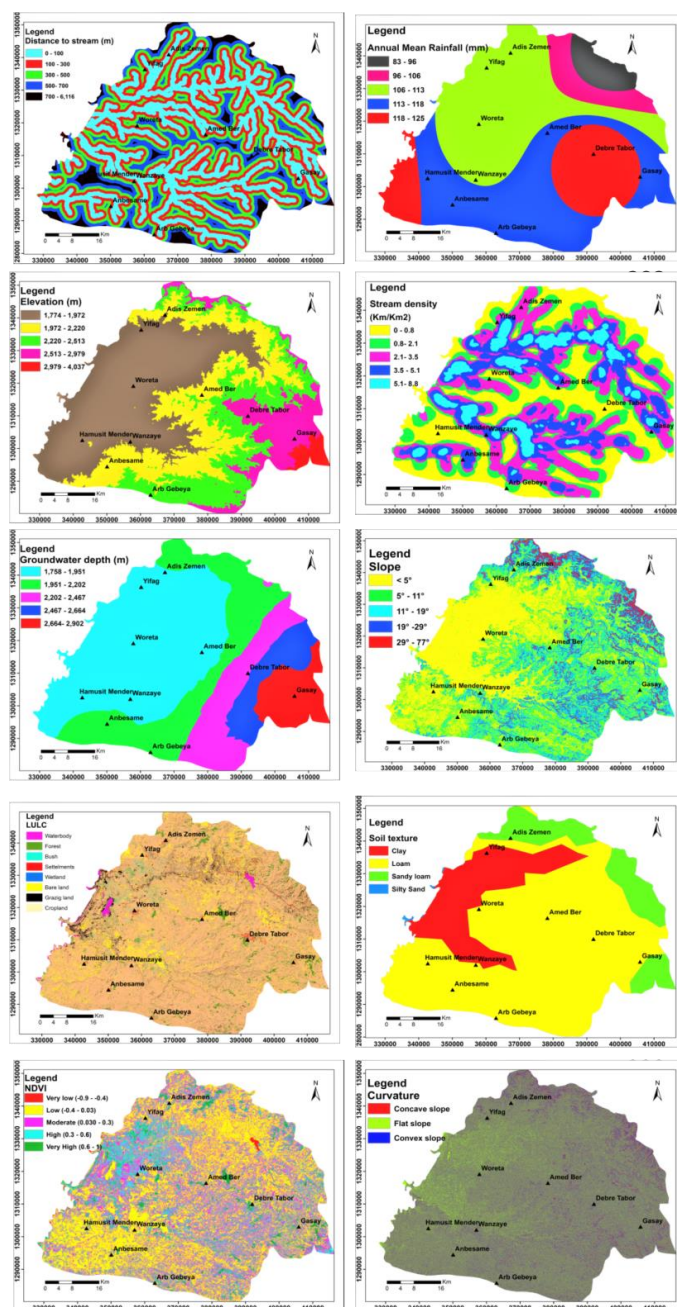


Figure 3 Flood governing factor maps



## 227     **Methodology**

228     To achieve the goal of the present research work, various activities and steps are employed. These  
 229     are data collection, Flood inventory mapping, database creation for Flood factors, Flood  
 230     susceptibility modeling using frequency ratio, information value, logistic regression, and AHP  
 231     methods as well as model validation using the Receiver Operating Characteristics curve (ROC).  
 232     Moreover, appropriate data, including a topographic map, borehole data, Digital Elevation Model  
 233     (DEM) with 12.5 m resolution, historical flood events, soil type map, geological map, and  
 234     meteorological data were collected. These data were collected from the United States Geological  
 235     Survey (USGS), Amhara Water Well Drilling Enterprise (AWWDE), Field Survey, Google Earth  
 236     Imagery from the NASA, Ethiopian National Meteorological Agency, and the Geological Survey  
 237     of Ethiopia (GSE). The flood location of the study area identified using historical records, Google  
 238     Earth imagery analysis, and intensive field survey. This was classified into training and testing  
 239     flood datasets. The training flood datasets were used for model preparation, whereas the testing  
 240     flood datasets were used for model prediction accuracy evaluation. Based on the data availability,  
 241     local environmental conditions, data evaluation, literature, and local people interview, eleven  
 242     flood-driving factors were determined. The flood driving factor maps and flood inventory map  
 243     were prepared using ArcGIS 10.1.

244     Geodatabase building is one of the most fundamental elements in the flood susceptibility mapping.  
 245     Therefore, four databases were built for information value, logistic regression, frequency ratio, and  
 246     analytical hierarchy process (AHP) models. The frequency ratio, information value, and analytical  
 247     hierarchy process (AHP) database contain flood inventory and flood driving factors while the  
 248     logistic regression database contains flood and no flood points with eleven- weighted flood driving  
 249     factors. After the database was built, an evaluation of the relationship between flood and flood  
 250     factors as well as the determination of the statistical significance of each flood factor was the next  
 251     step in flood susceptibility mapping. Therefore, eleven flood factor maps reclassified into subclass  
 252     and overlaid with reclassified training flood datasets. Weight ratings for all flood factor classes  
 253     assigned statistically using Excel. These weighted maps rasterized-using lookup in spatial analyst.  
 254     After rasterized the factor maps, the flood susceptibility index maps were generated by the sum-  
 255     up of all raster maps using a raster calculator in Map Algebra. These maps (LSI) are classified into  
 256     a fivefold classification scheme: very low, low, moderate, high, and very high susceptibility classes  
 257     using natural breaks (Fig. 5, 6, 7, and 8). In the case of the logistic regression method, the study



area classified as training flood and non-flood points using GIS. Then, the weight of eleven factors has been extracted to generate logistic regression coefficients of each flood factor in SPSS, and finally, the flood susceptibility index of the area was generated using the logistic flood probability equation (Eq. 8) and GIS tools (Fig. 3). Finally, the accuracy of the four models evaluated using the prediction rate curve based on observed testing flood datasets (Fig. 9).

## Modeling Approaches

### Information Value Model

The information value method is one of the probabilistic methods of a bivariate statistical method, which is used to envisage the correlation between floods and flood factor classes (Sakar et al., 2006). The information values for each factor class determined through the combination of reclassified flood raster to reclassified flood factor raster based on the presence of flood in a given map unit. These values are important to define the role of each causal factor in classes for flood occurrence. This can calculate as in Eq.1.

$$IV = \ln\left(\frac{\text{Conditional probability (CP)}}{\text{Prior probability (PP)}}\right) = \frac{\frac{N_{fopix}}{N_{cpix}}}{\frac{N_{tfopix}}{N_{tcpix}}} \quad (1)$$

Where Conditional probability is the ratio of the pixel of a flood in class to the pixel of a class and prior probability is the ratio of the total number of pixels of flood to the total number of pixels of the study area.  $N_{fopix}$  is a flood pixel/area in a flood factor class.  $N_{tfopix}$  is the total area of a flood in the entire study area.  $N_{cpix}$  is the area of the class in the study area and  $N_{tcpix}$  is the total pixel area in the entire study area. When the  $IV > 0.1$ , the flood occurrence with the factor classes have a high correlation, means it will have a high probability of flood occurrence however when the  $IV < 0.1$  or  $IV < 0$ , it is a low correlation between flood factors and flood occurrence which indicate a low probability of flood occurrence. After calculated the information value for each flood factor class using Microsoft excel and GIS, the information value for each factor class assigned through the join in the ArcGIS tool. Then, the weighted flood factors rasterized using the lookup tool in spatial analysis, and the flood susceptibility index (LSI) of the study area calculated as in Eq. 2.



$$LSI = \sum_{i=1}^n IV_i X_i \quad (2)$$

$$LSI = IV * Slope raster + IV * drainage density + IV * groundwater depth + IV * rainfall + IV * NDVI + IV * flow accumulation + IV * aspect raster + IV * curvature raster + IV * soil raster + IV * Land use raster + IV * Distance to stream raster$$

Where LSI is the flood susceptibility index and IV is the information value of each factor class. The higher value of LSI has indicated a higher probability of flood occurrence.

### Logistic Regression Model

Logistic regression is one of the popular multivariate statistical analysis methods, which can be used to establish a multivariate regression relationship between the dependent and independent variables (Pradhan and Lee, 2010). Among other statistical methods, the logistic regression model has been proven one of the most reliable approaches for flood susceptibility mapping to determine the most flood influencing factors (Lulseged and Yamagishi, 2005; Chau and Chan, 2005; Lee and Sanbath, 2006; Chen and Wang, 2007; Ricki and Graf, 2009]. This model is advantageous, as it does not require normal distribution and it uses continuous or discrete variables. The difficulty of using the logistic regression model lies in the sample size selection of dependent and independent variables for flood susceptibility analysis. There are three ways of sampling flood and non-flood points (Zhag et al., 2017). The first way is using all data from all the study areas. However, this leads to an uneven proportion of non-flood and flood pixels, which incorporate a large volume of data in the analysis. Using all flood pixels with equal non-flood pixels is the second method, which also results in a less reliable output, but it can reduce sample size and sampling bias. The third method uses an unequal or equal proportion of flood and non-flood pixels by classifying flood into training and testing datasets.

In the present work, the floods of the study area were classified into training flood datasets (70%) and as testing flood datasets (30%). In this study, the dependent data are a binary variable and are made up of 0 and 1, which represent the absence and presence of floods, respectively. Consequently, an equal number of non-flood sample points, whose dependent variable value is 0 where randomly selected from flood-free areas to represent the absence of floods using GIS. The



equal number of flood points and non-flood points were merged. Moreover, all the values of independent variables containing flood and non-flood were extracted from the maps of each flood governing factors using ArcGIS. Then, the logistic regression was conducted and coefficients were calculated in the SPSS program. It can be expressed mathematically (Lee and Sambath, 2006; Schicker and Moon, 2012) as:

$$P = \frac{1}{1 + e^{-z}} \quad \text{--- (3)}$$

Where P is the probability of flood occurrence that varies from zero to one. Z is the linear combination of the predictors and varies from  $-1 < z < 0$  for higher odds of non-flood occurrence to  $0 < z < 1$  for odds of higher flood occurrence. Z can be defined as:

$$Z = \beta_0 + \beta_1 X_1 + \beta_2 X_2 + \beta_3 X_3 \dots \beta_n X_n \quad \text{--- (4)}$$

Where  $x_1, x_2, x_3 \dots x_n$  are independent variables,  $\beta_0$  is the intercept of the slope of logistic regression analysis, and  $\beta_1, \beta_2, \beta_3 \dots \beta_n$  are the coefficients of the logistic regression analysis.

### Frequency Ratio Model

It is one of the bivariate probability methods, which is applicable to determine the correlation between flood occurrence and flood causative factor classes. The frequency ratio is the ratio of areas where the flood occurred in the areas to areas in which flood has not occurred. When the ratio value is greater than one, it indicates the strong correlation between factor class and flood occurrence in a given terrain, however, the ratio value less than one indicated that weak correlation between flood occurrence and flood factors, which means a low probability of flood occurrence (Lee and Talib, 2005). It can calculate using Eq. 5.

$$FR = \frac{a}{b} = \frac{\frac{N_{fopix}}{N_{tfopix}}}{\frac{N_{cpix}}{N_{tcpix}}} \quad \text{(5)}$$

Where FR is frequency ratio,  $N_{fopix}$  is a flood pixel/area in a flood factor class,  $N_{tfopix}$  is the total area of a flood in the entire study area (a),  $N_{cpix}$  is an area of the class in the study area and  $N_{tcpix}$  is the total pixel area in the entire study area (b). In the present research work, the frequency ratio for each causative factor class calculated using Eq.5, and the results summarized in Table 1.





After calculated the frequency ratio for each flood factor class using Microsoft Excel and GIS, the frequency ratio value for each factor class assigned through the join in the ArcGIS tool. Then the weighted flood factors rasterized using the lookup tool in spatial analysis. The flood susceptibility index (LSI) of the study area was calculated by carefully summing up the weighted factor raster maps using Eq. 6 by the raster calculator in Map Algebra of the spatial analysis tool. To get the flood susceptibility index, the frequency ratio of each factor type or class is summed as in Eq. 6. The flood susceptibility index indicated the degree of susceptibility of the area for flood occurrence.

$$LSI = \sum_{i=1}^n FR_i X_i \quad (6)$$

$$LSI = FR * Slope raster + FR * drainage density + FR * groundwater depth + FR * rainfall + FR * NDVI + FR * flow accumulation + FR * aspect raster + FR * curvature raster + FR * soil raster + FR * Land use raster + FR * Distance to stream raster$$

Where LSI is the flood susceptibility index, n is the number of flood factors,  $X_i$  is the flood factor and  $FR_i$  is the frequency ratio of each flood factor type or classes. After the flood susceptibility index was calculated, the index values were classified into a different level of flood susceptibility zones using natural breaks in the ArcGIS tool. The higher the value of the flood susceptibility index (LSI), the higher the probability of flood occurrence, but the lower the LSI indicates, the lower the probability of flood occurrence.

Based on the natural break classification, the flood susceptibility map of the study area has five classes such as very low, low, moderate, high, and very high landslide susceptibility class (Fig. 5).

#### **Analytical Hierarchy Process (AHP)**

The AHP is one of the qualitative methods used to determine the relationship between flood factor class and flood occurrence. The AHP method is a structured tool that is used to analyze difficult decisions based on the mathematics and psychology (Cho et al., 2015; Nguyen et al., 2015; Saaty, 2000; Zhang et al., 2016). To produce weighting factors, the pairwise comparison method was used by considered Saaty's ranking scale (Luu et al., 2018; Saaty, 2008). The consistency of calculated weight for each flood factor class was examined by the consistency ratio, which is



calculated by Eq.7 (Luu et al., 2018; Saaty, 2001). When the consistency ratio (CR) is less than 0.1, the weight of factor class that is calculated using the comparison matrix is consistent but if it is greater than 0.1, the comparison matrix is inconsistent and it should be revised. After the weight of each factor class was determined, the flood susceptibility map was produced as showed in Eq.9 (Rahmati et al., 2016c).

$$CR = \frac{CI}{RI} \quad (7) \quad CI = \frac{\lambda_{max} - n}{n} \quad (8)$$

$$FSI = \sum_{i=1}^n W_i * X_n \quad (9)$$

$$LSI = W * Slope raster + W * drainage density + W * groundwater depth + W * rainfall + W * NDVI + W * flow accumulation + W * aspect raster + W * curvature raster + W * soil raster + W * Land use raster + W * distance to stream raster$$

Where CR is consistency ratio, CI is consistency index, RI is the average random consistency index of the judgment matrix and  $\lambda_{max}$  is the largest eigenvalue derived from the paired comparison matrix and n is the number of flood factor,  $W_i$  is the weight of the flood factor,  $X_n$  is the flood factors and FSI is flooded susceptibility index.

## Result and Discussion

### Correlation of Flood Factors and Flood Incidence

#### Frequency Ratio Results

The frequency ratio method is used to calculate FR for each subclass of every flood-driving factor, which is the ratio of flood occurrence ratio to the area ratio. The result of the FR is summarized in Table 1. The greater the value of FR indicates a strong correlation between flood factor class and flood occurrence, a higher probability of flood occurrence when FR greater than unity (Table 1 and Fig. 4). As the results of the analysis designated in Table 1 and Fig. 4), the FR value for the first slope class,  $0^\circ - 5^\circ$  is greater than 1, is indicating a higher probability of flood occurrence which has 96% of a flooded area in the slope classes. This finding is consistent with other studies (e.g., Rahmati and Pourghasemi, 2017; Tehrany et al., 2014; Shafizadeh et al., 2018). However, the slope gradient greater than  $5^\circ$  has less correlation with flood occurrence. This result confirmed that the concepts as the slope gradient increase, the probability of flood occurrence in a given train



will be decreased. Because the steeper the slope gradient, the higher will be the rate of downslope water velocity however the lower the water concentration as well as the infiltration of rainwater into the ground. Nevertheless, when the slope gradient decreases, the potential for surface water concentration and rainwater infiltration into the ground will increase it depends on the hydraulic behavior of soil in that region. The higher concentration of surface water will have resulted in a high probability of flood incidence.

Slope curvature is another flood factor, which has three classes including Convex, Concave, and flat slope shapes. As the results of the correlation analysis of curvature class with flood inventory indicated in Table 1, the flat class received a higher FR value, indicating a strong correlation with flood occurrence. 56.1 % of the flooded area is fall in this class. This is because of the higher potential of rainwater concentration and low infiltration of rainwater due to its flatness and the existence of impermeable soil formation. Hence, this class is flat; the overflow of the water from the riverbed is high in a class that is why the flat portion of the curvature class indicating higher flood occurrence probability. This finding is confirmed with the other studies (Cao et al., 2016; Chapi et al., 2017; Khosravi et al., 2016; Shafizadeh et al., 2018).

Table 1 indicated that the FR value for elevation class is decreased as the elevation of the region is increased (Shafizadeh et al., 2018), indicating higher flood probability correlation with the first class of 1, 774 – 1, 972 m which is 99 % of the flooded area fall in this region. As indicated in Table 1, the relationship between elevation and the relative likelihood of flood occurrence is a negative correlation at the elevation > 1,972 m, meaning the probability of flood occurrence is low in elevated lands than low lands (Shafizadeh et al., 2018). This result is similar to the previous studies of (Hong et al., 2016; Shafizadeh et al., 2018).

In the spatial prediction of flood-prone areas in a catchment, distance to the river is a critical factor because floods occur due to the overflowing of water from the riverbanks (Chapi et al., 2017). Therefore, the areas closer to the riverbeds demonstrate a rapid response to rainstorms and flooding. As the results of the analysis shown in Table 1, the first four classes (0 -100 m, 100 – 300 m, 300 – 500 m, and 500 – 700 m) indicating a strong correlation with flood occurrence and 57.1 % of flooded area falls in these classes but the value of FR is decreased as the distance to the river bed is increased. This result confirmed that the concepts, the closer to the riverbed, the higher would be flood occurrence probability (Chapi et al., 2017; Hong et al., 2020; Shafizadeh et al.,



2018). As the correlation analysis of flow accumulation with flood inventory results indicated in Table 1, flow accumulation is one of the most important parameters in flood susceptibility mapping (Pradhan, 2010). The higher value of FR for flow accumulation is indicating higher concentration water and consequently higher flood occurrence probability. As Table 1 indicated, when the flow accumulation increased, the FR value is increased in parallel. Land use and land cover are other important parameters in flood susceptibility mapping which can be influenced by the interrelationship between surface and groundwater, the amount of infiltration, surface water concentration, and overland flow. As the result of land use and flood inventory correlation analysis indicated in Table 1, River zone, barren land, grazing land, settlement, and moderate vegetation/cropland have higher FR value, indicating higher flood occurrence probability. 37% of flooded area falls in these land-use classes. Because the moderate vegetation/cropland favors rainwater infiltration and hence the groundwater of this region is shallow, which enhanced the overland flow of water that is why moderate vegetation class has received higher FR value. The urban and grazing land have received higher FR value because of the impermeable nature of the class and indicating higher flood occurrence probability correlation. This result is in line with the work of (Shafizadeh et al., 2018). The NDVI is one of the important parameters for flood susceptibility mapping, its value ranges from  $-1$  to  $1$ . When the value is closer to one, the higher vegetation cover but the closer to  $-1$  implies the lower vegetation cover. Higher NDVI indicated dense vegetation that can reduce and slow water flow (Turoglu and Dolek, 2011). This gives the water time to infiltrate into the ground and resulting in a decrease in water volume and less probability of flood occurrence. However, it depends on the hydraulic behavior of soil and the depth of groundwater. In this study, the NDVI value ranges from  $-1$  to  $1$  which is from non-vegetated to highly vegetated regions. As the vegetation density increased, the flood susceptibility of a region will be decreased depending on the depth of groundwater and vegetation type. As the results of NDVI with flood inventory correlation analysis indicated in Table 1, the first, third, fourth, and fifth classes of the NDVI have received a higher value of FR and indicating higher flood occurrence probability correlation. This is because the groundwater depth of the study area is shallow which can be increased overland flow water by reducing the rate of infiltration of rainwater that is why the region shows higher flood occurrence correlation. 60.4% of the flooded area falls in these classes. Table 1 shows, as a stream density increased, the value of FR is increased in parallel and indicating high flood occurrence probability (Chapi et al., 2017; Shafizadeh et al.,



455 2018). The stream density classes ( $3.5 - 5.1 \text{ m/km}^2$  and  $5.1 - 8.8 \text{ m/km}^2$ ) have received a high  
 456 value of FR, indicating a strong correlation with flood occurrence and 61.5 % of flooded area falls  
 457 in these classes.

458 The amount of surface water concentration and rainwater infiltration rate mainly depends on the  
 459 hydraulic behavior of soils in the region. When the soil mass in a region is highly pervious, the  
 460 rate of water infiltration into the ground would be higher but the amount of surface water  
 461 concentration would be lower. This will enhance the non-flood incidence probability in a region.  
 462 However, this will be highly affected by the depth of groundwater. The results of flood inventory  
 463 with soil correlation analysis indicated in Table 1, silty sand and clay soil mass have received  
 464 higher value of FR compared to loam and sandy loam soil masses, indicating higher flood  
 465 incidence probability. This is because of the impervious behavior of fine-grained soils. When the  
 466 grain size of soil mass increased, the percent of pore space in between soil grain will increase but  
 467 the pore space diameter will low. This leads to the blockage of flowing water inside the soil. These  
 468 types of soil will have a high water holding capacity. This again increased the overland flow of  
 469 water. This can be contributed to high flood incidence probability. 88% of the flooded area falls  
 470 in the silty sand and clay soil masses. Table 1 indicated the shallow groundwater class has received  
 471 a high value of FR, indicating high flood incidence probability. 97.2 % of the flooded area falls in  
 472 very shallow groundwater depth. Even though rainfall is one of the most important flood driving  
 473 factors, its effect highly depends on the nature of the ground and the depth of the river channel. As  
 474 a result of rainfall with flood inventory analysis indicated in Table 1, the annual mean rainfall of  
 475 class (106 – 113 mm) has received a high value of FR, indicating high flood incidence probability.  
 476 This is because of the impervious hydraulic behavior of soil mass, low slope gradient, and shallow  
 477 groundwater depth. 68.5 % of the flooded area falls in the class (106 – 113 mm).

478

479

480



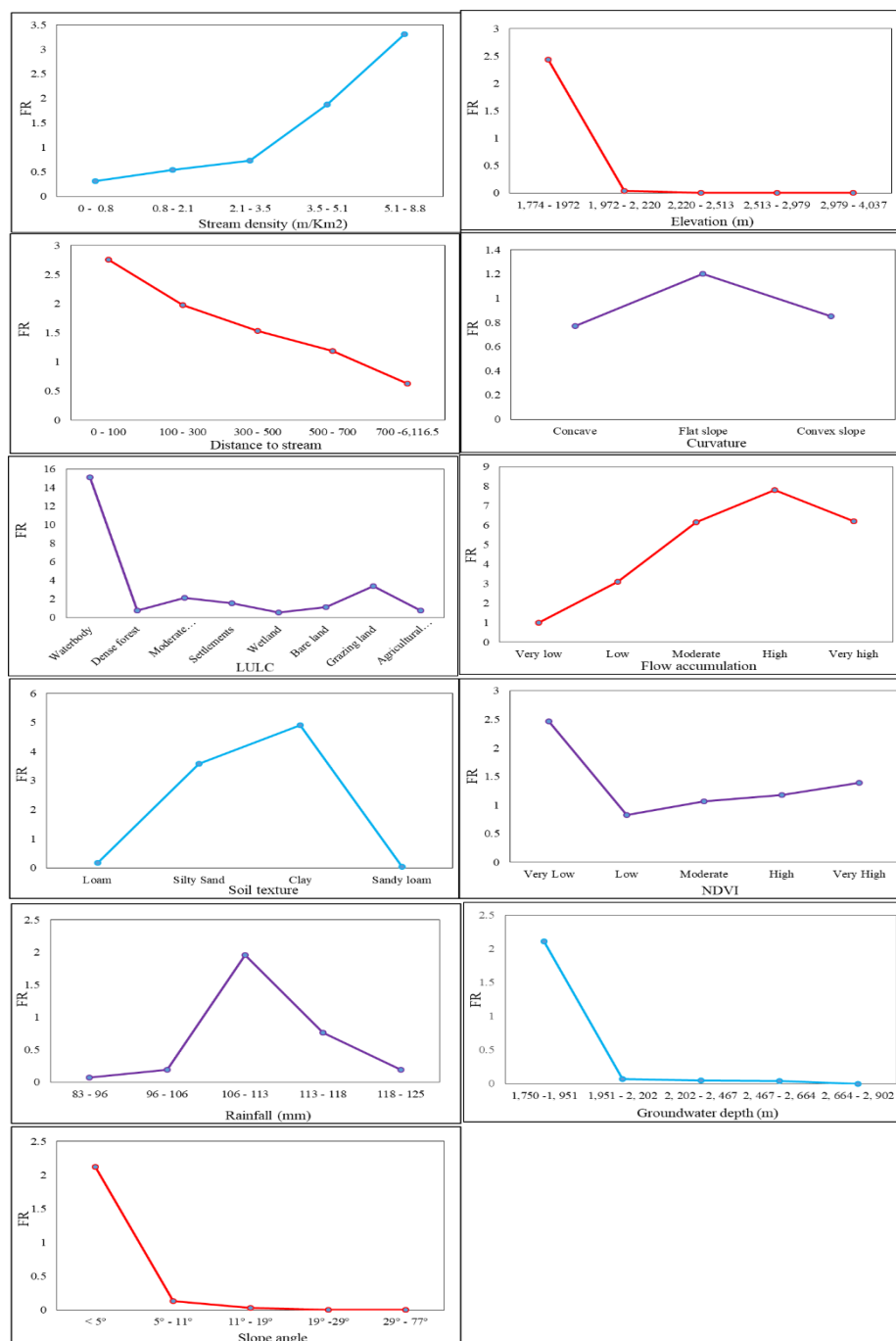


Figure 4 Statistical relationship between flood occurrence and flood driving factors



507

## 508 Information value Results

509 ArcGIS 10.2 and Microsoft Excel were used to calculate the information value (IV) of each factor  
 510 classes to determine the statistical significance of each factor class for flood incidence probability.  
 511 The factor class, which received higher (positive) information value indicating higher flood  
 512 occurrence probability, but the factor class, which has received lower (negative) information value  
 513 indicating a negative or weak correlation with flood occurrence probability. For example, as the  
 514 result shown in Table 1, the distance to the stream of the first four classes indicating a positive  
 515 correlation with flood occurrence but the rest factor class of the distance to stream, show negative  
 516 correlations for flood occurrence probability. The slope class  $> 5^\circ$ , elevation  $> 1,972$  m, the first  
 517 class of flow accumulation, distance to stream class  $> 700$  m, the stream density classes (0 – 0.8  
 518  $\text{Km}^2$ , 0.8 – 2.1  $\text{Km}^2$ , and 2.1 – 3.5  $\text{Km}^2$ ), slope curvature (concave & convex slope), LULC (dense  
 519 forest, wetland, and agriculture land), the second and the third classes of NDVI, Soil texture (sandy  
 520 loam & loam), and groundwater depth  $> 1,951$  m did show negative statistical correlation with  
 521 flood occurrence probability (Table 1).

522 Table 1 Statistical analysis results of flood occurrence and flood factors using FR, and IV methods

Slope Class	Class Pixel	% Class Pixel (b)	Flooded Area Pixel	% Flooded Area (a)	FR = a/b	Con_P	Prio_P	Con_P/Prio_P	IV = ln(Con_P/Prio_P)
$< 5^\circ$	1142672	45.18	507460	95.99	2.12	0.044	0.02	2.12	0.75
$5^\circ - 11^\circ$	6780625	26.81	18543	3.51	0.13	0.003	0.02	0.13	-2.03
$11^\circ - 19^\circ$	4173258	16.50	2457	0.46	0.03	0.001	0.02	0.03	-3.57
$19^\circ - 29^\circ$	2159660	8.54	207	0.04	0.00	0.000	0.02	0.00	-5.38
$29^\circ - 77^\circ$	750796	2.97	8	0.00	0.00	0.000	0.02	0.00	-7.58
<b>Elevation</b>									
Class (m)	Class Pixel	% Class Pixel (b)	Flooded Area Pixel	% Flooded Area (a)	FR = a/b	Con_P	Prio_P	Con_P/Prio_P	IV = ln(Con_P/Prio_P)
1,774 - 1972	1023774	40.48	523039	98.93	2.44	0.051	0.02	2.44	0.89
1,972 - 2,220	6383841	25.24	5292	1.00	0.04	0.001	0.02	0.04	-3.23
2,220 - 2,513	5148369	20.36	344	0.07	0.00	0.000	0.02	0.00	-5.75
2,513 - 2,979	3038070	12.01	0	0.00	0.00	0.000	0.02	0.00	
2,979 - 4,037	483038	1.91	0	0.00	0.00	0.000	0.02	0.00	
<b>Flow Accumulation</b>									
Class	Class Pixel	% Class Pixel (b)	Flooded Area Pixel	% Flooded Area (a)	FR = a/b	Con_P	Prio_P	Con_P/Prio_P	IV = ln(Con_P/Prio_P)
Very low	2525027	99.84	524941	99.29	0.99	0.021	0.02	0.99	-0.01
Low	25502	0.10	1653	0.31	3.10	0.065	0.02	3.10	1.13
Moderate	8076	0.03	1037	0.20	6.14	0.128	0.02	6.14	1.82
High	3257	0.01	532	0.10	7.81	0.163	0.02	7.81	2.06
Very high	3956	0.02	512	0.10	6.19	0.129	0.02	6.19	1.82
<b>Distance to Stream</b>									
Class (m)	Class Pixel	% Class Pixel (b)	Flooded Area Pixel	% Flooded Area (a)	FR = a/b	Con_P	Prio_P	Con_P/Prio_P	IV = ln(Con_P/Prio_P)
0 - 100	1310596	5.18	75517	14.28	2.76	0.058	0.02	2.76	1.01



100 - 300	2399920	9.49	99494	18.82	1.98	0.041	0.02	1.98	0.68
300 - 500	2288224	9.05	73168	13.84	1.53	0.032	0.02	1.53	0.43
500 - 700	2153831	8.52	53693	10.16	1.19	0.025	0.02	1.19	0.18
700 - 6,116.5	1713849 0	67.77	226803	42.90	0.63	0.013	0.02	0.63	-0.46
<b>Stream Density</b>									
Class (Km2)	Class Pixel	% Class Pixel (b)	Flooded Area Pixel	% Flooded Area (a)	FR = a/b	Con_P	Prio_P	Con_P/Prior_P	IV = ln(Con_P/Prio_P)
0 - 0.8	6882039	27.92	46291	8.76	0.31	0.007	0.02	0.31	-1.16
0.8 - 2.1	4983095	20.21	58174	11.00	0.54	0.012	0.02	0.54	-0.61
2.1 - 3.5	6317902	25.63	99289	18.78	0.73	0.016	0.02	0.73	-0.31
3.5 - 5.1	4350662	17.65	174722	33.05	1.87	0.040	0.02	1.87	0.63
5.1 - 8.8	2118013	8.59	150199	28.41	3.31	0.071	0.02	3.31	1.20
<b>Slope Curvature</b>									
Class	Class Pixel	% Class Pixel (b)	Flooded Area Pixel	% Flooded Area (a)	FR = a/b	Con_P	Prio_P	Con_P/Prior_P	IV = ln(Con_P/Prio_P)
Concave	4388463	17.35	71032	13.44	0.77	0.016	0.02	0.77	-0.26
Flat slope	1184002 2	46.82	296510	56.09	1.20	0.025	0.02	1.20	0.18
Convex slope	9062576	35.83	161133	30.48	0.85	0.018	0.02	0.85	-0.16
<b>LULC</b>									
Class name	Class Pixel	% Class Pixel (b)	Flooded Area Pixel	% Flooded Area (a)	FR = a/b	Con_P	Prio_P	Con_P/Prior_P	IV = ln(Con_P/Prio_P)
Waterbody	170378	0.67	53875	10.19	15.13	0.316	0.02	15.13	2.72
Dense forest	1584350	6.27	25202	4.77	0.76	0.016	0.02	0.76	-0.27
Moderate forest	185078	0.73	8200	1.55	2.12	0.044	0.02	2.12	0.75
Settlements	291928	1.15	9189	1.74	1.51	0.031	0.02	1.51	0.41
Wetland	72446	0.29	812	0.15	0.54	0.011	0.02	0.54	-0.62
Bare land	2288296	9.05	52119	9.86	1.09	0.023	0.02	1.09	0.09
Grazing land	1017397	4.02	71962	13.61	3.38	0.071	0.02	3.38	1.22
Agricultural land	1967877 9	77.82	307316	58.13	0.75	0.016	0.02	0.75	-0.29
<b>NDVI</b>									
Class	Class Pixel	% Class Pixel (b)	Flooded Area Pixel	% Flooded Area (a)	FR = a/b	Con_P	Prio_P	Con_P/Prior_P	IV = ln(Con_P/Prio_P)
Very Low	101398	0.26	3352	0.63	2.47	0.033	0.01	2.47	0.90
Low	1876229 5	47.48	209315	39.59	0.83	0.011	0.01	0.83	-0.18
Moderate	1157186 6	29.28	165084	31.23	1.07	0.014	0.01	1.07	0.06
High	6389220	16.17	100817	19.07	1.18	0.016	0.01	1.18	0.17
Very High	2692708	6.81	50107	9.48	1.39	0.019	0.01	1.39	0.33
<b>Soil Texture</b>									
Class	Class Pixel	% Class Pixel (b)	Flooded Area Pixel	% Flooded Area (a)	FR = a/b	Con_P	Prio_P	Con_P/Prior_P	IV = ln(Con_P/Prio_P)
Loam	1742444 5	68.91	61780	11.69	0.17	0.004	0.02	0.17	-1.77
Silty Sand	33442	0.13	2502	0.47	3.58	0.075	0.02	3.58	1.27
Clay	4514511	17.85	462543	87.50	4.90	0.102	0.02	4.90	1.59
Sandy loam	3313428	13.10	1809	0.34	0.03	0.001	0.02	0.03	-3.65
<b>Groundwater</b>									
Class	Class Pixel	% Class Pixel (b)	Flooded Area Pixel	% Flooded Area (a)	FR = a/b	Con_P	Prio_P	Con_P/Prior_P	IV = ln(Con_P/Prio_P)
1,750 - 1,951	1164396 4	46.04	514021	97.23	2.11	0.044	0.02	2.11	0.75
1,951 - 2,202	6130330	24.24	9137	1.73	0.07	0.001	0.02	0.07	-2.64
2,202 - 2,467	3367218	13.31	3792	0.72	0.05	0.001	0.02	0.05	-2.92
2,467 - 2,664	2064256	8.16	1725	0.33	0.04	0.001	0.02	0.04	-3.22
2,664 - 2,902	2085293	8.25		0.00	0.00	0.000	0.02	0.00	



Rainfall									
Class	Class Pixel	% Class Pixel (b)	Flooded Area Pixel	% Flooded Area (a)	FR = a/b	Con_P	Prio_P	Con_P/Prio_P	IV = ln(Con_P/Prio_P)
83 - 96	1207382	4.77	1763	0.33	0.07	0.001	0.02	0.07	-2.66
96 - 106	1641787	6.49	6480	1.23	0.19	0.004	0.02	0.19	-1.67
106 - 113	8856030	35.02	362318	68.53	1.96	0.041	0.02	1.96	0.67
113 - 118	8706231	34.42	139032	26.30	0.76	0.016	0.02	0.76	-0.27
118 - 125	4879631	19.29	19082	3.61	0.19	0.004	0.02	0.19	-1.68

IV is information value, FR is frequency ratio, a is flooded area in a factor class, b is an area of factor class, Con\_P is conditional probability and Prio\_P is the prior probability

523

## 524 Logistic Regression Results

525 Hence, sets of independent variables are so sensitive for collinearity (interrelatedness of  
 526 independent variable) which can be checked using Tolerance (TOL) and variance inflation factor  
 527 index (VIF), Multicollinearity test was applied using SPSS software before logistic regression  
 528 analysis. When the Tolerance (TOL) < 0.2 and VIF > 5, the given independent variable have  
 529 multicollinearity. As a result of the multicollinearity test indicated in Table 2, no independent  
 530 variables that were used in flood susceptibility analysis showed any multicollinearity. Using  
 531 logistic regression analysis in SPSS, the logistic regression coefficient for all flood-driving factors  
 532 was determined. Similar to the information value method, the positive logistic regression  
 533 coefficients indicating a positive association with flood occurrence probability but the negative  
 534 logistic regression coefficients indicating a negative correlation of flood factors with flood  
 535 occurrence probability. As the result of logistic regression analysis indicated in Table 2, Stream  
 536 density, NDVI, Rainfall, and Curvature have received negative logistic regression coefficients but  
 537 the remain factors that have received positive logistic regression coefficients, indicating the flood  
 538 factors have positively associated with flood occurrence probability.

539 Table 2 logistic coefficients of flood factors and multicollinearity statistics

		Collinearity Statistics	
Factors	LR Coefficients( $\beta$ )	Tolerance (TOL)	Variance inflation factor index (VIF)
Curvature	-0.04	0.983	1.017
Elevation	0.804	0.441	2.267
Flow Accumulation	0.222	0.957	1.045
Groundwater Depth	0.006	0.485	2.062
LULC	0.159	0.947	1.056
NDVI	-1.198	0.925	1.081
Rainfall	-0.148	0.652	1.534
Slope	0.769	0.608	1.644
Soil Texture	0.106	0.58	1.724



Distance to Stream	1.73	0.61	1.641
Stream Density	-0.095	0.65	1.538
Constant	-4.383		

540

## 541 **AHP Pairwise Comparison Matrix Results**

542 After reclassifying and ranking of the eleven-flood factor thematic raster into subclasses, the  
 543 pairwise comparison was performed for 5 x 5, 8 x 8, 4 x 4 and 3 x 3 matrixes using AHP calculator  
 544 (Table 3), where the diagonal element is equal to 1. As indicated in Table 3, the significance of  
 545 sub-criteria for each factor has shown in the row of the pairwise comparison matrix. The first row  
 546 in the Table 3 illustrates the significance of the first slope angle compared to the other slope angle  
 547 classes. For instance, the first slope angle class ( $0^{\circ} - 5^{\circ}$ ) is significantly more important than the  
 548 other slope classes, which are placed in the column for flood probability and assigned 9. However,  
 549 for the last classes of the slope angle at the row has less significant for flood probability and  
 550 assigned the reciprocal values of the pairwise comparison (E.g.  $1/9$  for the last slope class,  $29^{\circ} -$   
 551  $77^{\circ}$ ). The details for all parameters weight rating have summarized in Table 3 and the consistency  
 552 of the factor class weight was evaluated using the consistency ratio (CR). When  $CR < 0.1$ , the  
 553 weights' consistency is affirmed. As indicated in Table 3, the CR value for all factor classes is less  
 554 than 0.1 and indicated no weights' inconsistency. Based on the results of the pairwise comparison  
 555 analysis, as the slope angle, elevation, and groundwater depth increased, the flood probability will  
 556 be decreased and the vise verse. Similarly, as the distance to Riverbed increased, the flood  
 557 probability will be decreased. Concerning the other parameters, as the stream density, rainfall and  
 558 flow accumulation increased, the flood probability will be increased (Table 3). The flood  
 559 occurrence probability and its impact also depend on the hydraulic behavior of soil regard to the  
 560 other parameters. If the permeability of soil is high, the flood probability will low. This depends  
 561 on the grain size and diameters of pore space between soil particles. Therefore, the clay soil has  
 562 low permeability than high water holding capacity. This is the case why the clay soil has received  
 563 high value (9) in the pairwise comparison matrix (Table 3). In the study area, Settlement, bare  
 564 land, agricultural land, grazing land, water body, and wetland have a high contribution to flood  
 565 occurrence respectively compared to the forested regions.

566





567 Table 3 Pairwise comparison matrix and weight of flood factor classes

Factors	Sub Factor Class(i)	Sub Factor Class (j)					
	Class	0° - 0.5°	0.85° - 11°	11° - 19°	19° - 29°	29° - 77°	W
Slope	0° - 5°	1	2	5	7	9	0.509
	5° - 11°	0.5	1	2	3	4	0.229
	11° - 19°	0.2	0.5	1	2	5	0.143
	19° - 29°	0.14	0.33	0.5	1	2	0.075
	29° - 77°	0.11	0.25	0.2	0.5	1	0.044
	Consistency Ratio CR = 5.9%						
Elevation	Class (m)	1,774 - 1972	1,972 - 2,220	2,220 - 2,513	2,513 - 2,979	2,979 - 4,037	W
	1,774 - 1972	1	3	6	7	9	0.543
	1,972 - 2,220	0.33	1	3	3	4	0.222
	2,220 - 2,513	0.17	0.33	1	2	5	0.123
	2,513 - 2,979	0.14	0.33	0.5	1	2	0.071
	2,979 - 4,037	0.11	0.25	0.2	0.5	1	0.042
	Consistency Ratio CR = 1.4%						
Flow	Class	Very low	Low	Moderate	High	Very high	W
	Very low	1	0.33	0.11	0.11	0.11	0.031
	Low	3	1	0.33	0.33	0.33	0.092
	Moderate	9	3	1	0.33	0.33	0.186
	High	9	3	3	1	1	0.346
	Very high	9	3	3	1	1	0.346
	Consistency Ratio CR = 4.4%						
Distance Stream	Class (m)	0 - 100	100 - 300	300 - 500	500 - 700	700 - 6,116.5	W
	0 - 100	1	3	5	9	9	0.529
	100 - 300	0.33	1	3	3	5	0.229
	300 - 500	0.2	0.33	1	3	7	0.147
	500 - 700	0.11	0.33	0.33	1	1	0.053
	700 - 6,116.5	0.11	0.2	0.14	1	1	0.042
	Consistency Ratio CR = 6.5%						
Stream Density	Class (Km2)	0 - 0.8	0.8 - 2.1	2.1 - 3.5	3.5 - 5.1	5.1 - 8.8	W
	0 - 0.8	1	0.33	0.2	0.14	0.11	0.033
	0.8 - 2.1	3	1	0.33	0.2	0.14	0.064
	2.1 - 3.5	5	3	1	0.33	0.14	0.124
	3.5 - 5.1	7	5	3	1	1	0.324
	5.1 - 8.8	9	7	7	1	1	0.455
	Consistency Ratio CR = 5.9%						
NDVI	Class	Very Low	Low	Moderate	High	Very High	W
	Very Low	1	2	5	9	9	0.489
	Low	0.5	1	3	5	7	0.282
	Moderate	0.2	0.33	1	3	7	0.144
	High	0.11	0.2	0.33	1	1	0.047
	Very High	0.11	0.14	0.14	1	1	0.039
	Consistency Ratio CR = 4.4%						
Rainfall	Class	83 - 96	96 - 106	106 - 113	113 - 118	118 - 125	W
	83 - 96	1	0.5	0.2	0.11	0.11	0.033
	96 - 106	2	1	0.33	0.2	0.14	0.057
	106 - 113	5	3	1	0.33	0.14	0.123
	113 - 118	9	5	3	1	1	0.335
	118 - 125	9	7	7	1	1	0.452
	Consistency Ratio CR = 4.4%						
GW	Class (m)	1,750 - 1,951	1,951 - 2,202	2,202 - 2,467	2,467 - 2,664	2,664 - 2,902	W
	1,750 - 1,951	1	3	5	9	9	0.522
	1,951 - 2,202	0.33	1	3	5	7	0.256



	2, 202 - 2, 467	0.2	0.33	1	3	7				<b>0.139</b>
	2, 467 - 2, 664	0.11	0.2	0.33	1	1				<b>0.046</b>
	2, 664 - 2, 902	0.11	0.14	0.14	1	1				<b>0.038</b>
	<b>Consistency Ratio CR = 5.3%</b>									
	Class	Waterbody	Dense Forest	Moderate Forest	Settlement	Wetland	Bare land	Grassing land	Agricultural land	<b>W</b>
<b>LULC</b>	Waterbody	1	4	4	0.33	2	0.5	0.5	0.33	<b>0.091</b>
	Dense Forest	0.25	1	0.5	0.2	0.14	0.11	0.11	0.11	<b>0.021</b>
	Moderate Forest	0.25	2	1	0.2	0.33	0.11	0.11	0.11	<b>0.027</b>
	Settlement	3	5	5	1	3	1	2	2	<b>0.225</b>
	Wetland	0.5	7	3	0.33	1	0.5	0.5	0.33	<b>0.08</b>
	Bare land	2	9	9	1	2	1	2	1	<b>0.204</b>
	Grassing land	2	9	9	0.5	2	0.5	1	1	<b>0.16</b>
	Agricultural land	3	9	9	0.5	3	1	1	1	<b>0.192</b>
	<b>Consistency Ratio CR = 3.9%</b>									
<b>Soil</b>	Class	Loam	Silty Sand	Clay	Sandy loam	<b>W</b>				
	Loam	1	3	0.11	4	<b>0.148</b>				
	Silty Sand	0.33	1	0.11	2	<b>0.07</b>				
	Clay	9	9	1	9	<b>0.735</b>				
	Sandy loam	0.25	0.5	0.11	1	<b>0.047</b>				
	<b>Consistency Ratio CR = 8.9%</b>									
<b>Curvature</b>	Class	Concave	Flat slope	Convex slope	<b>W</b>					
	Concave	1	0.5	0.5	<b>0.196</b>					
	Flat slope	2	1	2	<b>0.493</b>					
	Convex slope	2	0.5	1	<b>0.311</b>					
	<b>Consistency Ratio CR = 5.6%</b>									

569

## 570 Flood Susceptibility Model

### 571 Frequency Ratio Flood Susceptibility model

572 After weight rating for each flood driving factor classes using FR, each flood-driving factor was  
 573 converted into raster using lookup in spatial analysis option under ArcGIS 10.2 software. The flood  
 574 Susceptibility index of the study area is generated by sum up all raster maps carefully using the  
 575 raster calculator in spatial analysis. The flood susceptibility index (Fig. 5) was reclassified into  
 576 five classes (Very low, low, moderate, high, and very high) using the natural break method in  
 577 ArcGIS as shown in Eq. 6. As a result, shown in Table 4, high and very high flood susceptibility  
 578 classes have covered 19.8 % and 20.7 % of the study area, respectively. However, the remaining,  
 579 14.1 %, 23.6 %, and 21.7 % of the study area covered by very low, low, and moderate flood  
 580 susceptibility areas. The high and very high flood susceptibility classes in the study area fell closer  
 581 to the Ribb River, Gumara River, Ribb dam, and other streams as well as flat and impervious soil  
 582 regions. However, the low and very low regions fell in the steep slope gradient and deep  
 583 groundwater depth as well as densely forested and previous regions.



584  $FSI = FR * Slope \text{ raster} + FR * Stream \text{ density raster} + FR * Slope \text{ curvature raster} + FR * Soil$   
 585  $Texture \text{ raster} + FR * Land \text{ use raster} + FR * Distance \text{ to stream raster} + FR * Flow \text{ Accumulation}$   
 586  $+ FR * Groundwater \text{ depth raster} + FR * Elevation \text{ raster} + FR * NDVI \text{ raster} + FR * Rainfall \text{ raster}.$

### 587 **Information Value Flood Susceptibility Model**

588 Similar to the frequency ratio method, the flood susceptibility index generated using the  
 589 information value method (Fig. 6) was reclassified into five classes (Very low, low, moderate,  
 590 high, and very high) using the natural break method in ArcGIS as shown in Eq. 2. As a result,  
 591 shown in Table 4, high and very high flood susceptibility classes have covered 20.3 % and 20.2 %  
 592 of the study area, respectively. However, the remaining, 13.1 %, 23.9 %, and 22.5 % of the study  
 593 area covered by very low, low, and moderate flood susceptibility areas.

594  $FSI = IV * Slope \text{ raster} + IV * Stream \text{ density raster} + IV * Slope \text{ curvature raster} + IV * Soil \text{ Texture}$   
 595  $\text{raster} + IV * Land \text{ use raster} + IV * Distance \text{ to stream raster} + IV * Flow \text{ Accumulation} +$   
 596  $IV * Groundwater \text{ depth raster} + IV * Elevation \text{ raster} + IV * NDVI \text{ raster} + IV * Rainfall \text{ raster}$

### 597 **Logistic Regression Flood Susceptibility Model**

598 In the logistic regression method, logistic regression coefficients for individual factor was  
 599 determined using SPSS. The linear combination of LR constant and factor products with LR  
 600 coefficients is called Z, which is calculated as shown Eq. 4. The value of Z enters into Eq. 3 and  
 601 the flood probability index (P) was generated. The value of P is range from 0 – 1 and the closer  
 602 the value to one is indicating the higher flood susceptibility region. Similar to the frequency ratio  
 603 and information value methods, the flood susceptibility index generated using the logistic  
 604 regression method (Fig. 7) was reclassified into five classes (Very low, low, moderate, high, and  
 605 very high) using the natural break method in ArcGIS as shown in Eq. 3. As a result, shown in  
 606 Table 4, high and very high flood susceptibility classes have covered 13.2 % and 9.3 % of the  
 607 study area, respectively. However, the remaining, 54.3 %, 11.2 %, and 12.1 % of the study area  
 608 covered by very low, low, and moderate flood susceptibility area.

609  $Z = -4.38 + 0.769 * Slope \text{ raster} + -0.095 * Stream \text{ density raster} + -0.040 * Slope \text{ curvature raster}$   
 610  $+ 0.106 * Soil \text{ Texture raster} + 0.159 * Land \text{ use raster} + 1.73 * Distance \text{ to stream raster}$   
 611  $+ 0.222 * Flow \text{ Accumulation} + 0.006 * Groundwater \text{ depth raster} + 0.804 * Elevation \text{ raster} +$   
 612  $1.198 * NDVI \text{ raster} + -0.148 * Rainfall \text{ raster}$



## 613 Analytical Hierarchical Process Flood Susceptibility Model

614 Similar to the frequency ratio and information value methods, the flood susceptibility index  
 615 generated using the analytical hierarchical process method (Fig. 8) was reclassified into five classes  
 616 (Very low, low, moderate, high, and very high) using the natural break method in ArcGIS as shown  
 617 in Eq. 9. As a result, shown in Table 4, high and very high flood susceptibility classes have covered  
 618 19.8% and 10.2 % of the study area, respectively. However, the remaining, 19.7%, 24.8%, and  
 619 25.6% of the study area covered by very low, low, and moderate flood susceptibility areas.

$$\begin{aligned}
 620 \quad LSI = & W * Slope raster + W * drainage density + W * groundwater depth + W \\
 621 \quad & * rainfall + W * NDVI + W * flow accumulation + W * aspect raster + W \\
 622 \quad & * curvature raster + W * soil raster + W * Land use raster + W \\
 623 \quad & * distance to stream raster
 \end{aligned}$$

624 Table 4 Statistical model summary of FR, LR, IV, and AHP methods

IVFSI	Class	IVFSP	% FSM	VFP	% VF	LRFSI	LRFSP	% FSM	VFP	% VF
-25 - -15.1	Very low	3226367	13.1	13	0.01	0 - 0.1	13381271	54.3	627	0.34
-15.1 - -10	Low	5901361	23.9	472	0.26	0.1 - 0.3	2756345	11.2	4470	2.46
- 10 - -5	Moderate	5535540	22.5	4816	2.65	0.3 - 0.5	2972834	12.1	15071	8.28
-5 - 1.2	High	4996851	20.3	21844	12.00	0.5 - 0.7	3243717	13.2	61228	33.64
1.2 – 13	Very high	4982782	20.2	154863	85.09	0.7 - 1	2288737	9.3	100612	55.28
FRFSI	Class	FRFSP	% FSM	VFP	% VF	Methods	Success Rate Curve, AUC %		Prediction Rate Curve AUC %	
4 – 9	Very low	3480969	14.1	15	0.01	LR	75.6		81.4	
9 – 14	Low	5825312	23.6	511	0.28	FR	97.9		99.1	
14 - 19	Moderate	5356987	21.7	4775	2.62	IV	71		78.2	
19 - 27	High	4874089	19.8	21635	11.89					
27 - 46	Very high	5105544	20.7	155072	85.20	AHP		82.5		86.9
AHPFSI	Class	AHPFSP	%FSM	VFP	% VF					
0.5 - 1.7	Very low	4849344	19.7	0	0.00					
1.7 - 2.3	Low	6122024	24.8	12	0.01					
2.3 – 2.9	Moderate	6298368	25.6	558	0.31					
2.9 - 3.6	High	4887029	19.8	10491	5.76					
3,6 – 5.3	Very high	2486139	10.1	170947	93.92					

Note: AHPFSI is analytical hierarchy process flood susceptibility index, IVFSI is information value flood susceptibility index, IVFSP is information value flood susceptibility pixel, FSM is flood susceptibility map, VFP is validation flood pixel, VF is validation flood, LRFSI is logistic regression flood susceptibility index, LRFSP is logistic regression flood susceptibility pixel, FRFSI is frequency ratio flood susceptibility index, FRFSP is frequency ratio flood susceptibility pixel



## 625 4.2 Model Validation and Comparison

626 The most important ambition of flood susceptibility mapping is to determine the areas that are  
 627 prone to flood hazards. However, flood susceptibility modeling without predication and model  
 628 performance evaluation is non-sense to the application of disaster reduction programs. Although  
 629 researchers used many techniques to validate the flood susceptibility model, the receiver operating  
 630 characteristics (ROC) method is routinely used (Shafizadeh et al., 2018; Tehrany et al., 2013;  
 631 Liuzzo et al., 2019) because of its simplify and produce clear as well as reliable results (Samanta  
 632 et al., 2018; Rhmati et al., 2016; Khosravi et al., 2016; Pradhan and Lee, 2010). Therefore, the  
 633 prediction and model performance of flood susceptibility map of the study area was validated by  
 634 comparing the flood model with existing flood data using the ROC curve (Lee et al., 2007; Tien  
 635 Bui et al., 2012; Pourghasemi et al., 2012). The prediction accuracy and model performance of the  
 636 flood susceptibility map was evaluated quantitatively using the receiver operating characteristics  
 637 (ROC) curve based on the evaluation of the true and false positive rates (Chauhan et al., 2010;  
 638 Mahyat et al., 2019). Both the training and testing dataset were used to calculate the success rate  
 639 curve and predictive rate curve. The predictive rate curve for the four models was obtained by  
 640 comparing testing flood datasets with flood susceptibility index while the success rate curve also  
 641 obtained for the four models by comparing training flood datasets. The AUC value ranges from  
 642 0.5 – 1 (Yesilnacar and Topal, 2005) and the closer the value to one indicating the higher accuracy  
 643 of the model. As the results of the Success rate curve of AUC analysis indicated in (Table 4 and  
 644 Fig. 9), FR has received a 97.9% and 99.1% success rate curve and prediction rate curve,  
 645 respectively. When evaluating the accuracy of the model, the FR model indicated superior  
 646 performance (97.9%), followed by the AHP model (82.5%), LR model (75.6%), and then the IV  
 647 model (71%). Similarly, the model has the greatest prediction capacity (99.1%), followed by the  
 648 AHP model (86.9%), LR model (81.4%) and the IV model has 78.2%. From the AUC results, the  
 649 FR model indicating, the highest model accuracy and prediction capacity but the IV model has  
 650 indicated relatively less model accuracy and predictive capacity in the present study. Moreover,  
 651 the four models (FR, AHP, LR, and IV) resulted in  $AUC > 75\%$  which is good, very good, and  
 652 excellent model performance (Yesilnacar and Topal, 2005), respectively. This finding is similar to  
 653 the work of (Bui et al., 2018; Samanta et al., 2018a; Rahman et al., 2019). Besides the ROC curve,  
 654 flood-testing datasets that are not used for model development were overlaid on the four flood  
 655 susceptible maps. The number of flood points that falls in the very high susceptibility class was





measured as shown in Table 4, 85.2%, 55.3%, 85.1% and 93.92% of flood points were fell in very high susceptibility class of FR, LR, IV and AHP models. Here also the FR and AHP models confirms again its excellent performance followed by the IV model. All in all the flood points which fell in very high susceptibility class are greater than 55%, indicating acceptable model accuracy of IV, LR, AHP and FR models.

Although the analytical hierarchy process, frequency ratio, information value, and logistic regression methods are routinely used methods for flood susceptibility mapping, they have some foreseeable limitations. For example, the logistic regression model can perform multivariate statistical analysis between a dependent variable and a set of independent variables (Table 2), but it is incapable to analyze the impacts of internal classes of flood governing factors individually on flood occurrence. As the results indicated in Table 2, the importance of flood driving factors is determined using the LR model. The result showed that among eleven factors, distance to stream (1.73), elevation (0.8), slope gradient (0.769), flow accumulation (0.222), land use (0.159), soil texture (0.106), and groundwater depth (0.006) had received the highest statistical impact on the probability of flood occurrence (Table 2). These are in line with the finding of Kia et al., 2012; Chapi et al., 2017; Mosavi et al., 2018; Falah et al., 2019; Rahman et al., 2019). Overall, logistic regression also causes oversimplification and generalization on the effects of flood governing factors. Whereas frequency ratio and information value are simple and effective statistical methods that can extract the influence of each flood governing factor class on flood occurrence (Table 1), but it cannot consider the relationship between these flood governing factors and flood occurrence. The analytical hierarchy process method is very important methods to evaluate the effects of factors and factor classes on flood occurrence probability, however, this method has a series of subjectivity problem during pairwise comparison to assign the weights for each factor class and flood driving factors. In summary, there is no unique statistical and expert based methods to determine both the effects of each factor classes and general effects of flood factors. Therefore, a combination use of bivariate and multivariate statistical methods to predict flood susceptibility in a region is very essential when there is no a unique method that help to evaluate the effects of flood driving factors as general and inherently.

In literature, comparison among information value, logistic regression, frequency ratio and analytical hierarchy process method was not performed rather than the frequency ratio method



with the information value method, logistic regression method with information value and frequency methods, the AHP method with the information value method, and the AHP method with the frequency ratio method. (Chen et al., 2016) states that the prediction rate of 83.69% using the frequency ratio model is better than the prediction rate of 81.22% using the information value method. This finding is similar to the present study, the frequency ratio method showed better performance for both success rates (AUC = 97.9%) and predictive rate curve (AUC = 99.1%) than the information value method with success rate curve (AUC = 71.0%) and predictive rate curve (AUC = 78.2%). As shown from the work of (Mahyat et al., 2018), the logistic regression model showed a high predictive accuracy of AUC value of 79.45 % compared to the frequency ratio and information value model with prediction rate curve value (AUC = 67.33% for FR, AUC = 78.18% for IV). Nevertheless, in the present model, the frequency model showed a relatively few difference in prediction rate value (AUC = 99.1 %) than the information value and logistic regression models with prediction rate value (AUC = 78.2% for IV, AUC = 81.4% for LR). From the work of (Khosravi et al., 2016), based on the predictive rate value of the area under the receiver operating characteristic curve (AUC), the frequency ratio (FR) and analytical hierarchy process (AHP) models showed a little bit different in predictive capacity, which is 96.57% for the FR model and 94.92% for the AHP model. This result is in line with the present work, the prediction rate of 99.1% using the frequency ratio model is better performance than the prediction rate curve 86.9% for the AHP model. Rahman et al., (2019) found that the logistic regression model (AUC = 86.8%) gave a more realistic flood susceptibility map than the frequency ratio (AUC = 85.6%) and AHP (AUC = 64%) model. However, this result is not in line with the present work which is the frequency ratio is better than AHP and the logistic regression model. This difference happens mostly due to the number of and types of input parameters for model construction. Generally, the AHP, bivariate, and multivariate statistical methods in literature and this study showed, the closer prediction capacity with AUC > 64% and AUC > 75%, respectively fell in the range of good and very good/excellent performance (Yesilnacar and Topal, 2005). The flood validation results for the four models (FR, LR, IV & AHP) are closer to each other. Therefore, from these results, the research work finds out that in flood susceptibility mapping, the four models have equal potential to generate flood-prone areas but factor selection should be playing a more important role than the methods. Although all statistical models indicated higher prediction accuracy, based on their statistical significance analysis result of AUC value (see Table ), the



frequency ratio (FR) model is better than the analytical hierarchy process (AHP), logistic regression (LR) model, and information value model for regional land use planning, flood hazard mitigation, and prevention purposes.

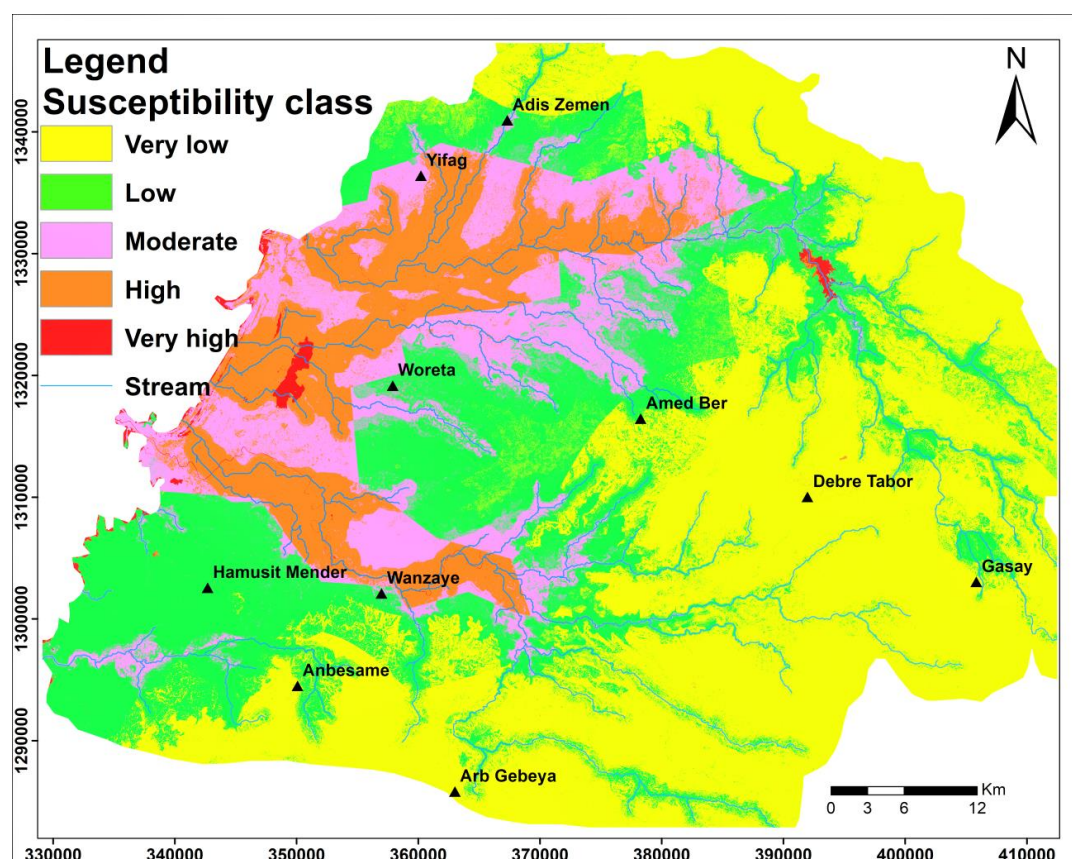


Figure 5 Flood Susceptibility map using frequency ratio method

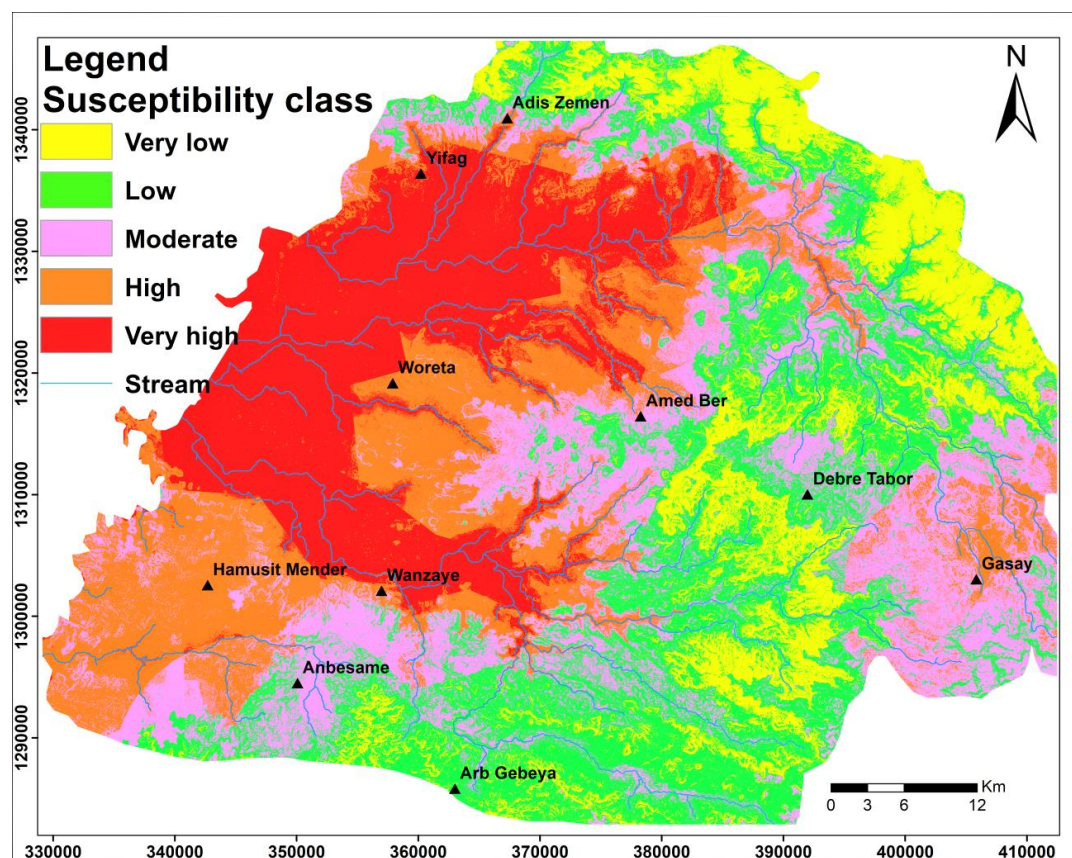
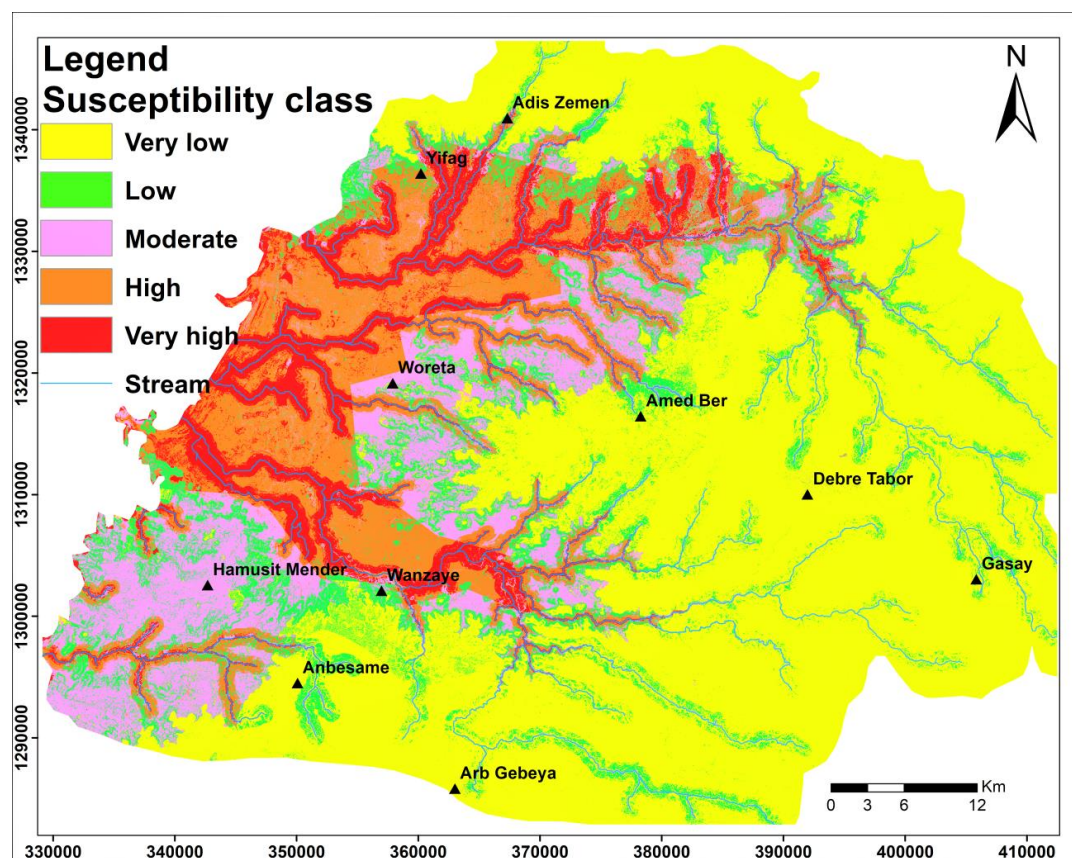


Figure 6 Flood Susceptibility map using information value method





726

727 Figure 7 Flood Susceptibility map using logistic regression method

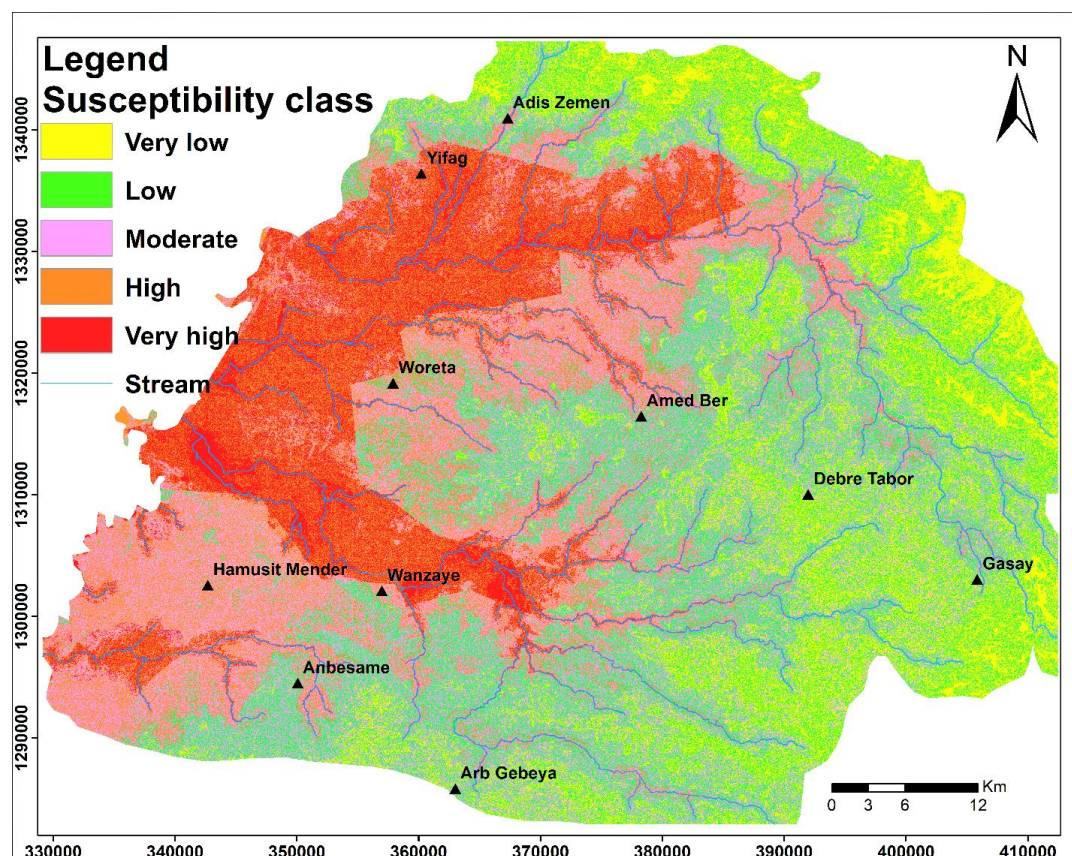
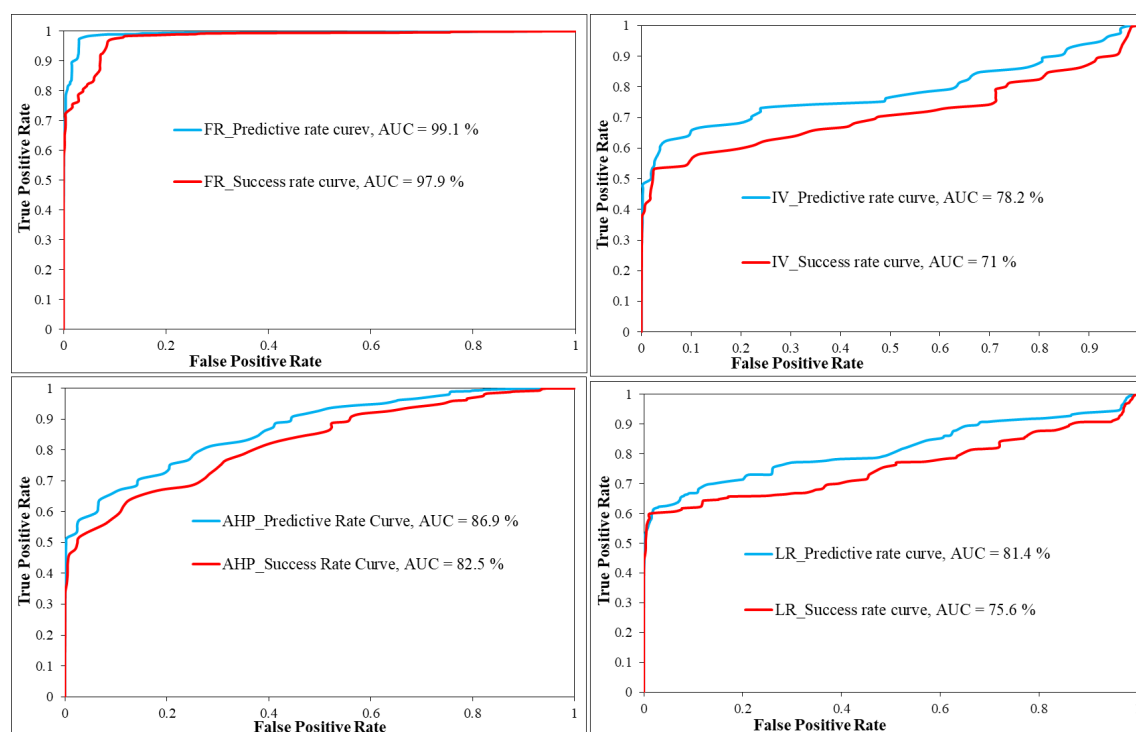


Figure 8 Flood Susceptibility map using analytical hierarchy process method



734  
 735 Figure 9 Predictive and success rate curves for IV, LR, FR and AHP methods

736

## 737 Conclusion

738 In flood hazard reduction and mitigation management, flood susceptibility map is one of the key element.  
 739 Therefore, it is essential to prepare the most precise and reliable flood susceptibility map. The application  
 740 of frequency ratio, information value, logistic regression, and analytical hierarchy process (AHP) models  
 741 have been tested in flood susceptibility mapping and their results are compared to each other using AUC  
 742 results. The results showed that the flood susceptibility map produced by the frequency ratio method is  
 743 relatively better than the AHP, logistic regression, and information value methods. However, the ranges of  
 744 prediction accuracy value for all four methods are indicated that the frequency ratio, AHP, logistic  
 745 regression, and information value methods are capable to produce an acceptable flood susceptibility model.  
 746 The models, which are generated using the bivariate, multivariate statistical, and AHP models, can  
 747 help to understand the flood hazard problems in the study area. Although the resulting maps cannot  
 748 forecast the time, and how often it can occur, it has provided the spatial distribution of flood  
 749 probability. These models can also provide important information to the researchers, local people,





750 government, and planners to reduce the flood hazard problems in the study area. Therefore, the  
751 concerned bodies may at the Wereda/District, Zone, Region, and Federal levels take tangible  
752 activities to mitigate the flood problem by avoiding permanent activities at the high and very high  
753 regions with the integration of construction of check dams for streams.

754

#### 755 **Author contributions**

756 Azemeraw Wubalem has conceptualized statistical analysis and done the completed modeling  
757 analysis. Azemeraw Wubalem wrote the original drafts, which was reviewed and edited by all co-  
758 authors. All authors have their contributions to writing the manuscript.

#### 759 **Competing interest**

760 We declare that we do not any conflict of interest.

#### 761 **Acknowledgments**

762 We would like to thank the University of Gondar for financial and equipment supports. We also  
763 would like to thank all contributing project partners. We also want to give our special thanks to  
764 the West Amhara Meteorological Agency, Amhara Water Well Drilling Enterprise, and Ethiopian  
765 Mapping Agency.

766

767

768

769

770

771

772



## 773 Reference

- 774 Adger, N.W.: Vulnerability, *Glob. Environ. Chang.*, 16, 268–281, 2006.
- 775 Ayalew, L, Yamagishi, H.: The application of GIS-based logistic regression for landslide  
 776 susceptibility mapping in the Kakuda- Yahiko Mountains, Central Japan, *Geomorphology*, 65,  
 777 15 – 31, 2005.
- 778 Bednarik, M, Yilmaz, I, Marschalko, M.: Landslide hazard and risk assessment: a case study  
 779 from the Hlohovec–Sered’ landslide area in south-west Slovakia, *Nat Hazards*,  
 780 DOI:10.1007/s11069-012-0257-7, 2012.
- 781 Calil, J, Beck, MW, Gleason, M, Merrifield, M, Klausmeyer, K, Newkirk, S.: Aligning natural  
 782 resource conservation and flood hazard mitigation in California, *PLoS One*, 10, 1–14,  
 783 <https://doi.org/10.1371/journal.pone.0132651> PMID: 26200353, 2015.
- 784 Cao, C, Xu, P, Wang, Y, Chen, J, Zheng, L, Niu C.: Flash flood hazard susceptibility mapping  
 785 using frequency ratio and statistical index methods in coalmine subsidence areas, *Sustainability*,  
 786 8(9), 948, 2016.
- 787 Celikyilmaz, A, Turksen, IB.: Modeling uncertainty with fuzzy logic, *Stud Fuzziness Soft*  
 788 *Comput*, 240, 149– 215, 2009.
- 789 Chandak, P.G., Sayyed, S.S., Kulkarni, Y.U., Devtale, M.K.: Landslide hazard zonation  
 790 mapping using information value method near Parphi village in Garhwal Himalaya, *Ljemas*, 4,  
 791 228 – 236, 2016.
- 792 Chapi, K, Singh, VP, Shirzadi, A, Shahabi, H, Bui, DT, Pham, BT, Khosravi, K.: A novel hybrid  
 793 artificial intelligence approach for flood susceptibility assessment, *Environ Modell Softw*, 95,  
 794 229–245, 2017.
- 795 Chau, K. T, Chan, J. E.: The regional bias of landslide data in generating susceptibility maps  
 796 using logistic regression: Case of Hong Kong Island, *Landslide*, 2, 280–290, 2005.
- 797 Chauhan, S, Sharma, M, Arora, MK.: Landslide susceptibility zonation of the Chamoli region,  
 798 Garhwal Himalayas, using a logistic regression model, *Landslides* 7, 411–423, 2010.



- 799 Chen, Z, Wang, J.: Landslide hazard mapping using a logistic regression model in Mackenzie  
 800 Valley, Canada, Nat. Hazards, 42,75–89, 2007.
- 801 Chen, Z., and Wang, J.: Landslide hazard mapping using a logistic regression model in  
 802 Mackenzie Valley, Canada, Nat. Hazard, 42(1), 75-89, 2007.
- 803 Cho, S, Kim, J, Heo, E.: Application of fuzzy analytic hierarchy process to select the optimal  
 804 heating facility for Korean horticulture and stockbreeding sectors, Renew Sustain Energy Rev,  
 805 49,1075–1083, 2015.
- 806 Dai, F. C. and Lee, C. F.: Landslide characteristics and slope instability modeling using GIS,  
 807 Lantau Island, Hong Kong, Geomorphology, 42, 213-228, 2002.
- 808 Das, G, Lepcha, K.: Application of logistic regression (LR) and frequency ratio (FR) models  
 809 for landslide susceptibility mapping in Relli Khola river basin of Darjeeling Himalaya. India,  
 810 SN Appl Sci., 1,1453, <https://doi.org/10.1007/s42452-019-1499-2>, 2019.
- 811 Donati, L, and Turrini, M. C.: An objective method to rank the importance of the factors  
 812 predisposing to landslides with the GIS methodology application to an area of the Apennines  
 813 (Valnerina; Perugia, Italy), Engg. Geol., 63, 277-289, 2002.
- 814 Duman, T.Y., Can, T., Gokceoglu, C., Nefeslioglu, H. A., and Sonmez, H.: Application of  
 815 logistic regression for landslide susceptibility zoning of Cekmese area, Istanbul, Turkey, Verlag,  
 816 242 – 256, 2006.
- 817 Falah, F, Rahmati, O, Rostami, M, Ahmadisharaf, E, Daliakopoulos, IN, Pourghasemi, HR.:  
 818 Artificial neural networks for food susceptibility mapping in data-scarce urban areas. In:  
 819 Pourghasemi HR, Gokceoglu C (eds) Spatial modeling in GIS and R for the earth and  
 820 environmental sciences, Elsevier, 323–336, 2019.
- 821 Hong, H, Junzhi, L, A-Xing, Z.: Modeling landslide susceptibility using logit Boost alternating  
 822 decision trees and forest by penalizing attributes with the bagging ensemble, Science of the  
 823 Total Environment, 718:3-15, <https://doi.org/10.1007/s00477-012-0598-5>, 2020.



- 824 Jacinto, R., Grosso, N., Reis, E., Dias, L., Santos, F.D., Garrett, P.: Continental Portuguese  
 825 Territory Flood Susceptibility Index—Contribution to a vulnerability index, *Nat. Hazards Earth*  
 826 *Syst. Sci.*, 15, 1907–1919, 2015.
- 827 Khosravi, K., Nohani, E., Maroufinia, E., Pourghasemi, HR.: A GIS-based flood susceptibility  
 828 assessment and its mapping in Iran: a comparison between frequency ratio and weights-of  
 829 evidence bivariate statistical models with multi-criteria decision-making technique, *Nat*  
 830 *Hazards*, 83, 1–41, 2016.
- 831 Kia, MB, Pirasteh, S, Pradhan, B, Mahmud, AR, Sulaiman, WNA, Moradi, A.: An artificial  
 832 neural network model for flood simulation using GIS: Johor River Basin, Malaysia, *Environ*  
 833 *Earth Sci.*, 67, 251– 264, <https://doi.org/10.1007/s12665-011-1504-z>, 2012.
- 834 Kouhpeima, S. Feizniab, H. Ahmadib, Moghadamniab, A.R.: Landslide susceptibility mapping  
 835 using logistic regression analysis in Latyan catchment, *Desert*, 85 – 95, 2017.
- 836 Lee, MJ, Kang, JE, Jeon, S.: Application of frequency ratio model and validation for predictive  
 837 flooded area susceptibility mapping using GIS, In: *Geoscience and Remote Sensing*  
 838 *Symposium (IGARSS)*, IEEE International, Munich, 895–898, 2012.
- 839 Lee, M-J, Kang, J-e, Jeon, S.: Application of frequency ratio model and validation for predictive  
 840 flooded area susceptibility mapping using GIS, *Proceedings of the Geoscience and Remote*  
 841 *Sensing Symposium (IGARSS)*, Jul 22–27; Munich (Germany): IEEE International, 4, 2012.
- 842 Lee, S, Pradhan, B.: Landslide hazard mapping at Selangor, Malaysia using frequency ratio and  
 843 logistic regression models, *Landslides*, 4, 33–41, 2007.
- 844 Lee, S, Sambath, T.: Landslide susceptibility mapping in the Damrei Romel area, Cambodia  
 845 using frequency ratio and logistic regression models, *Environ. Geol.*, 50, 847– 855, 2006.
- 846 Lee, S, Talib, JA.: Probabilistic landslide susceptibility and factor effect analysis, *J Environ*  
 847 *Geol.*, 47, 982–990, 2005.
- 848 Liuzzo, L, Sammartano, V, Freni, G.: Comparison between Different Distributed Methods for  
 849 Flood Susceptibility Mapping, *Water Resour Manag*, 33, 3155–3173,  
 850 <https://doi.org/10.1007/s11269-01902293-w>, 2019.



- 851 Luelseged Ayalew and Yamagishi H.: The application of GIS-based logistic regression for  
 852 landslide susceptibility mapping in the Kakuda- Yahiko Mountains, Central Japan,  
 853 *Geomorphology*, 65, 15 – 31, 2005.
- 854 Luu, C, Von Meding, J, Kanjanabootra, S.: Assessing food hazard using food marks and  
 855 analytic hierarchy process approach: a case study for the 2013 food event in Quang Nam,  
 856 Vietnam, *Nat Hazards*, 90,1031–1050, 2018.
- 857 Mahyat, Shafapour, Tehrany, Lalit, Kumar, Mustafa, Neamah, Jebur, Farzin Shabani.:  
 858 Evaluating the application of the statistical index method in flood susceptibility mapping and  
 859 its comparison with frequency ratio and logistic regression methods, *Geomatics, Natural*  
 860 *Hazards and Risk*, 10, 1, 79-101, DOI: 10.1080/19475705.2018.1506509, 2019.
- 861 Meten, M., Bhandary, N.P., and Yatabe, R. GIS-based frequency ratio and logistic regression  
 862 modeling for landslide susceptibility mapping of Debre Sina area in central Ethiopia, *J.Mt.Sci*,  
 863 12(6), 1355 – 1372, 2015.
- 864 Mosavi, A, Ozturk, P, Chau, K-w.: Flood prediction using machine learning models: literature  
 865 review, *Water*, 10, 1536, 2018.
- 866 Nguyen, AT, Nguyen, LD, Le-Hoai, L, Dang, CN.: Quantifying the complexity of  
 867 transportation projects using the fuzzy analytic hierarchy process, *Int J Project Manage*,  
 868 33,1364–1376, 2015.
- 869 Ohlmacher, GC, Davis, JC. Using multiple logistic regression and GIS technology to predict  
 870 landslide hazard in northeast Kansas, USA, *Eng Geol*, 69, 331–343, 2003.
- 871 Pham, BT, Prakash, I, Singh, S.K, Shizardi, A, Shahabi, H, Bui, D.T.: Landslide susceptibility  
 872 modeling using reduce error pruning trees and different ensemble techniques:hybrid machine  
 873 learning approach, *Catena*, 175:203-218, 2019b.
- 874 Pourghasemi, HR, Pradhan, B, Gokceoglu, C.: Application of fuzzy logic and analytical  
 875 hierarchy process (AHP) to landslide susceptibility mapping at Haraz watershed, Iran *Nat*  
 876 *Hazards*, 63, 965–996, 2012.



- 877 Pradhan, B, Mansor, S, Pirasteh, S, Buchroithner, M.: Landslide hazard and risk analyses at a  
 878 landslide-prone catchment area using the statistical-based geospatial model, *Int J Remote Sens*,  
 879 32(14), 4075–4087, DOI:10.1080/01431161.2010.484433, 2011.
- 880 Pradhan, B., Lee, S.: Landslide susceptibility assessment and factor effect analysis:  
 881 backpropagation artificial neural networks and their comparison with frequency ratio and  
 882 bivariate logistic regression modeling, *Environmental Modelling & Software*, 25, 747-759,  
 883 2010.
- 884 Rahman, M, Chen, Ningsheng, Md Monirul, Islam, Ashraf, Dewan, Javed, Iqbal,  
 885 Rana, Muhammad, Ali, Washakh, Tian, Shufeng.: Flood Susceptibility Assessment  
 886 in Bangladesh Using Machine Learning and Multi-criteria Decision Analysis, *Earth Systems*  
 887 *and Environment*, 3, 585–601, <https://doi.org/10.1007/s41748-019-00123-y>, 2019.
- 888 Rahmati, O, Pourghasemi, HR.: Identification of critical flood prone areas in data-scarce and  
 889 ungauged regions: a comparison of three data mining models, *Water Resour Manag* 31(5),  
 890 1473–1487, 2017.
- 891 Rahmati, O, Pourghasemi, HR, Zeinivand, H.: Flood susceptibility mapping using frequency  
 892 ratio and weights-of-evidence models in the Golastan Province, Iran, *Geocarto Int.*, 31: 42–70,  
 893 <https://doi.org/10.1080/10106049.2015.1041559>, 2016.
- 894 Regmi, A.D., Yoshida, K., Pourghasemi, H.R., Dhital, M.R., Pradhan, B.: Landslide  
 895 susceptibility mapping along Bhalubang-Shiwapur area of mid-western Nepal using frequency  
 896 ratio and conditional probability models, *Jour. Mountain Sci.*, 11(5), 1266-1285, 2014.
- 897 Rickli, C, Graf, F.: Effects of forests on shallow landslides – case studies in Switzerland, *Forest*  
 898 *Snow and Landscape Research*, 82, 33–44, 2009.
- 899 Saaty, TL.: Fundamentals of decision making and priority theory with the analytic hierarchy  
 900 process, Rws Publications, Pittsburgh, 6, 2000.
- 901 Saaty, TL.: The seven pillars of the analytic hierarchy process. In: Köksalan M, Zionts S (eds)  
 902 Multiple criteria decision making in the new millennium, Springer, Berlin, Heidelberg, 15–37,  
 903 2001.



- 904 Saaty, TL.: Decision making with the analytic hierarchy process, *Int J serv Sci*, 1, 83–98, 2008.
- 905 Samanta, RK, Bhunia, GS, Shit, PK, Pourghasemi, HR.: Flood susceptibility mapping using  
 906 geospatial frequency ratio technique: a case study of Subarnarekha River Basin, India, *Model*  
 907 *Earth Syst Environ*, 4, 395–408, <https://doi.org/10.1007/s40808-018-0427-z>, 2018.
- 908 Sarkar, S., Kanungo, D, Ptra, A., Kumar, P.: Disaster mitigation of debris flow, slope failure,  
 909 and landslides. GIS-based landslide susceptibility case study in Indian Himalaya, *Universal*  
 910 *Acadamy Press*, Tokyo, Japan, 617 – 624, 2006.
- 911 Sarkar, S., Rjan, Martha, T., and Roy, A.: Landslide susceptibility Assessment using  
 912 information value method in parts of the Darjeeling Himalayas, *Geological Society of India*,  
 913 82, 351– 362, 2013.
- 914 Schicker, R., Moon, V.: Comparison of bivariate and multivariate statistical approaches in  
 915 landslide susceptibility mapping at a regional scale, *Geomorphology*, 161-162, 40-57, 2012.
- 916 Shafizadeh-Moghadam H, Valavi R, Shahabi H, Chapi K, Shirzadi A. Novel forecasting  
 917 approaches using combination of machine learning and statistical models for flood  
 918 susceptibility mapping. *J Environ Manage.* 2018; 217: 1–11.  
 919 <https://doi.org/10.1016/j.jenvman.2018.03.089> PMID: 29579536
- 920 Tehrany, M, Jones, S.: Evaluating the variations in the flood susceptibility maps accuracies due  
 921 to the alterations in the type and extent of the flood inventory, *ISPRS-Int Arc Photogramm*,  
 922 *Remote Sens Spatial Inform Sci.*, 12, 209–214, 2017.
- 923 Tehrany, MS, Pradhan, B, Jebur, MN.: Spatial prediction of flood susceptible areas using rule  
 924 based decision tree (DT) and a novel ensemble bivariate and multivariate statistical models in  
 925 GIS, *J Hydrol*, 504, 69–79, 2013.
- 926 Tehrany, MS, Pradhan, B, Jebur, MN.: Flood susceptibility mapping using a novel ensemble  
 927 weights-ofevidence and support vector machine models in GIS, *J Hydrol*, 512,332–343, 2014.
- 928 Tien Bui, D, Pradhan, B, Lofman, O, Revhaug, I, Dick, OB.: Landslide susceptibility mapping  
 929 at Hoa Binh province (Vietnam) using an adaptive neuro-fuzzy inference system and GIS,  
 930 *Comput Geosci*, 45,199–211, 2012.





- 931 Turoğlu, H, Dölek, I.: Floods and their likely impacts on ecological environment in Bolaman  
 932 River basin (Ordu, Turkey), *RJAS*, 43(4), 167–173, 2011.
- 933 Wang, HB, Wu, SR, Shi, JS, Li, B.: Qualitative hazard and risk assessment of landslides: a  
 934 practical framework for a case study in China, *Nat Hazards*, DOI:10.1007/s11069-011-0008-1,  
 935 2011.
- 936 Wubalem, Azemeraw\*, Meten, M.: Landslide susceptibility mapping using information value  
 937 and logistic regression models in Goncha Siso Eneses area, northwestern Ethiopia. *SN Applied*  
 938 *Sciences*, Switzerland AG., 2, 807, <https://doi.org/10.1007/s42452-020-2563-0>, 2020.
- 939 Yesilnacar, E, Topal, T.: Landslide susceptibility mapping: A comparison of logistic regression  
 940 and neural networks method in a medium scale study, Hendek region (Turkey), *Engineering*  
 941 *Geology*, 79, 251 – 266, 2005.
- 942 Zhang, W, Lu, J, Zhang, Y.: Comprehensive evaluation index system of low carbon road  
 943 transport based on fuzzy evaluation method, *Procedia Eng*, 137, 659–668, 2016.
- 944 Zhang, YS., Javed, Igbol, Yae, Y.: Landslide susceptibility mapping using an integrated model  
 945 of information value and logistic regression methods in the Bailongjiang watershed, Gansu  
 946 province, China, *Journal of mountain science*, 14, 249 – 268, 2017.
- 947 Zou, Q, Zhou, J, Zhou, C, Song, L, Guo, J.: Comprehensive flood risk assessment based on set  
 948 pair analysis-variable fuzzy sets model and fuzzy AHP, *Stoch Environ Res Risk Assess*, 27,  
 949 525–546, 2013.
- 950